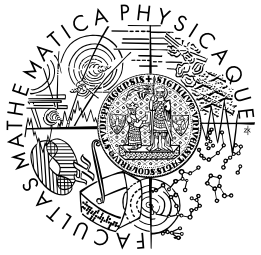

FACULTY
OF MATHEMATICS
AND PHYSICS
Charles University

MASTER THESIS

Dominik Černý

Asteroid models reconstructed from photometric data and stellar occultations

Astronomical Institute of Charles University

Supervisor of the master thesis: doc. Mgr. Josef Ďurech, Ph.D.

Study programme: Astronomy and Astrophysics

Study branch: FAAP

Prague 2024

I declare that I carried out this master thesis independently, and only with the cited sources, literature and other professional sources. It has not been used to obtain another or the same degree.

I understand that my work relates to the rights and obligations under the Act No. 121/2000 Sb., the Copyright Act, as amended, in particular the fact that the Charles University has the right to conclude a license agreement on the use of this work as a school work pursuant to Section 60 subsection 1 of the Copyright Act.

In ..... date ....

Author's signature

I would like to thank my supervisor Josef Ďurech for his patience and advice in writing this thesis. Also his colleague Josef Hanuš for his instructions. And all of occultation observers who provided data used in this thesis.

Title: Asteroid models reconstructed from photometric data and stellar occultations

Author: Dominik Černý

Institute: Astronomical Institute of Charles University

Supervisor: doc. Mgr. Josef Ďurech, Ph.D., Astronomical Institute of Charles University

Abstract: Asteroids are the most numerous group of bodies in our Solar System. However, our observations are limited because of their size and distance. Occultations allow us to determine the shape and size of even the smaller asteroids with kilometre precision. All observations of occultations are publicly available, but not generally used in the modelling of asteroids. Even thou occultations can scale models from light curves and solve their pole ambiguity, most models are created only from light curves. This thesis aims to implement occultations in the process of asteroids' modelling. In my bachelor thesis, I have scaled existing models for 274 asteroids thus determining their precise dimensions and solving the pole ambiguity in some cases. In this thesis, I have created new models using occultations. The occultations allow me to create new and more precise models than light curves alone with non-convex features, thus expanding our knowledge of asteroids.

Keywords: Asteroids Occultations Modelling

Contents

Introduction

Asteroids are an important part of our Solar System. However, they are small and relatively far, so we can get disc-resolved images for only the largest of them. For most of asteroids, we have only disc-integrated integrated observations like light curves and infrared (IR) observations. From these observations, we can determine the asteroid's orbit and get a first estimate of its size and shape. These values are not precise, because of the unknown albedo of the asteroid and imperfect thermal models. However, the knowledge of asteroid's, size, shape, and orbit is crucial to understand both the Solar System's history and its future, including predictions of the possible impact of asteroids on Earth. The orbits of asteroids tell us about their interaction with planets and their shape and spin about their mutual collisions. So by studying asteroids, we can learn a lot about collision processes which play a vital part in planetary systems formation. Therefore, we need observations of asteroids with good spatial resolution which are capable of showing non-convex features. This is what occultations enable.

The observations of occultations are based only on timing, not precise astrometry, so even amateur observers can achieve spatial precision in the order of kilometres. Sometimes even better. When the timing precision of observation is in the order of 0.01 s and the relative speed of the asteroid and Earth is in the order of 10 $\mathrm{km \cdot s^{-1}}$, then the final spatial resolution is in the order of 0.1 km. This allows us not only to find the precise dimensions of the asteroid but also to see some surface features, even for the smallest of asteroids.

The number of observations of occultations has been increasing in recent years as the precision of their predictions is improving. A few years ago, occultations were recorded for only a few asteroids, but now over a thousand new observations are made each year and this number is expected to rise. So with this increase in data set, occultations could become a basic part of asteroid study. Therefore, we need to process lots of observations for asteroids with and without an already existing model.

The goal of my work is to process all available data from occultation observation and use them to improve our knowledge about asteroids' shapes and sizes. Also to prepare a way for routine processing of occultation in the future. There are more than 16 000 models derived from light curve inversion in the Database of Asteroid Models from Inversion Techniques (DAMIT)[1] belonging to over 10 000 asteroids. Most of these models do not include precise dimensions, because of the unknown albedo, and most of them are convex. And because they are derived from light curves alone, they are often ambiguous in pole position. In my bachelor thesis (Černý, 2022) I have performed scaling of models for 274 asteroids to 516 observed occultations. Most of these asteroids (190) have a model in DAMIT that agrees with occultations, and I have been able to determine their dimensions and for some of them even solve the pole ambiguity. Another 44 asteroids had a model which I was not able to fit on occultations and 40 asteroids had unusable occultations. The asteroids that have non-fitting models are my primary subject in further study and candidates for new model creation.

Most models in DAMIT are derived solely from light curves without any use

[1] `https://astro.troja.mff.cuni.cz/projects/damit/`

of occultations. So by using the occultation observations in the model creation, I can get a more precise scaled model with non-convex surface features. Using both light curves and occultations in asteroid modelling allows me to improve shape solutions over the models from light curves alone, solve pole ambiguity in most cases, and add dimension with uncertainty to the model. I aim to enable routine processing of occultations in the modelling of asteroids and any observations that will become available after the model creation for its verification.

1. Asteroids

Asteroids (also called minor planets) are the most numerous group of bodies in the Solar System. Currently, there are over 1.3 million known asteroids. Most of these are located in the main belt between Mars and Jupiter at a distance of 2–3.3 AU from the Sun. The total mass of the main belt is around $4 \cdot 10^{-4}$ Earth mass, with over 35 % in the dwarf planet Ceres alone.

There are several other populations of asteroids. Among them are near–Earth objects (NEO), which are asteroids that have perihelia less than 1.3 AU. Some of these objects cross the path of the Earth and can potentially collide with it. Asteroids cannot stay in this region for long. Typically not more than 10 Myr, before they collide with some inner planet or fall into the Sun as a result of perturbation from these planets.

The fact that we observe NEOs today means that there exists some mechanism with which they are supplemented. The source of NEOs is the main belt from which asteroids are perturbed toward the inner Solar System. This process is driven by planets, mostly Jupiter and Saturn. The planets' gravitational resonances in the main belt cause changes in asteroids' eccentricity and migration of perihelia to the inner Solar System. But to get the asteroids close to the resonance, we need some other mechanism. The mechanism which can drive asteroids towards resonances is the Yarkovsky effect (Bottke et al., 2006). This effect is caused by a radiation force that acts on the body from its thermal emission. The strongest emission is from the hottest part of the body, which is not the sub-solar point but shifted because of asteroid rotation. The final force is then in the opposite direction and is partly transversal to the orbital motion, so it causes changes in the asteroid's semi-major axis. It can be shown that this mechanism can replenish the NEO and keep their population constant (Morbidelli and Vokrouhlický, 2003).

Smaller populations are Trojans, which move around Lagrangian points L4 and L5 of the Sun–Jupiter system. Another group is Centaurs, whose orbits lie among planets of the outer Solar System. These asteroids are probably migrating from trans-Neptunian areas towards the inner Solar System because they could not exist on their current orbits for long.

The most numerous group of asteroids are trans-Neptunian objects (TNO). Their orbits are beyond the orbit of Neptune and are therefore hard to observe. This is the reason we have more known asteroids in the main belt, although it has a smaller population.

Only the biggest asteroids are remnants from the early formation of protoplanetary disks when planets were created. Others have been reformed during later collisions. The processes that created planets in the Solar System have also influenced minor planets. So by studying asteroids, we can follow the history of our Solar System. Therefore, any model of the evolution of the Solar system has to be consistent with our observations of minor planets.

All of the minor planets' properties are important because each holds different information about asteroids' history. An asteroid's orbit indicates interaction with the planet, like collisions and gravitational disturbances. The shape, size and spin of the asteroids are influenced mostly by mutual interactions of minor

planets, especially collisions. From shapes and spins, we can derive collision history and processes in an asteroid belt. This way we can explore collision disruptions of asteroids, fragmentation laws, starting populations of asteroids (Holsapple, 2022), and creation of families (Novaković et al., 2022).

1.1 Asteroid observations

The most common type of observation available is astrometry measurements. These are measurements of point sources and their position in time. From these measurements, we can determine the orbit of the asteroid and predict its future positions.

Other important observations are photometric. They consist of measuring asteroid's brightness and its changes in time. The results of these measurements are light curves (dependence of brightness on time). Based on these data, we can determine the asteroid's rotational period, pole position, and shape.

The basic characteristic that we want to determine is the size of the asteroid. It could be determined by the absolute magnitude of incoming light from the asteroid to an observer, which is given by the reflecting surface and the asteroid's albedo. But because we usually do not know the albedo of asteroids, we cannot precisely determine asteroid size only from light curves.

Other possible asteroid observations are infrared measurements. In this case, the light from an asteroid is observed in a far infrared part of the spectrum usually by spacecraft. Earth-bound observations in the IR spectrum are limited because of the extinction in the atmosphere. This part of the spectrum is not influenced so much by albedo, because we do not measure reflected light from the Sun, but radiation from the asteroid itself. This depends on the asteroid's temperature and is characterized by thermal models. These models work with the mean value of observed light, so they can only describe asteroid size, not its shape because they assume the spherical shape of the asteroid. They also use assumptions about the thermal behaviour of the asteroids, which does not have to be precise, so the derived diameter is not precise. We can therefore get an estimate of the size of the asteroid, and then by using light curves we can get an estimate of the albedo (Delbo et al., 2015). The most widely used are standard thermal models (STM) (Lebofsky et al., 1986) and the Near-Earth Asteroid Model (NEATM)(Harris, 1998).

Observations using adaptive optics are probably the most precise way to determine asteroid's shape and size. But these observations are difficult and only possible for larger asteroids with more expensive instruments(Saint-Pe et al., 1993).

Radar observations can also give us information about an asteroid's size, shape, and rotation. The dimension can even be determined with precision in the order of dozens of meters. However, these observations are only possible for the closest asteroids. Examples of radar observation can be found in e.g. Magri et al. (2007)

None of these observations can give us precise dimensions for smaller asteroids in the main belt and further. That is the reason why occultations are really useful tools for minor planet observations. They can help us determine the precise dimensions and shapes of asteroids and require only basic observational equip-

ment. Even shape characteristics can be observed with accuracy in the order of kilometres. But in order for these observations to be useful, we need several observations per event to get two-dimensional spatial resolution, because each observation of occultation is just one-dimensional.

2. Stellar occultations

An occultation occurs when some object crosses the path of light coming to us from a distant star. Usually, we are talking about objects in our Solar System, which are smaller than the star, but also much closer, and their angular size is generally larger than that of the star. In that case, the object completely blocks the incoming light from the star and creates a moving shadow on Earth (Fig. 2.1). If there is an observer in the path of the shadow, they will see a temporary disappearance and reappearance of the star. From the timings of disappearance and reappearance of the occulted star, we can determine the width of the shadow by multiplying it by its velocity. This way, we get the width of the shadow at one point along its length. If there are more observers in the shadow path, preferably in different positions across the path, we can reconstruct the shadow's shape and with it the projection of the occulting object, (Fig. 2.2).

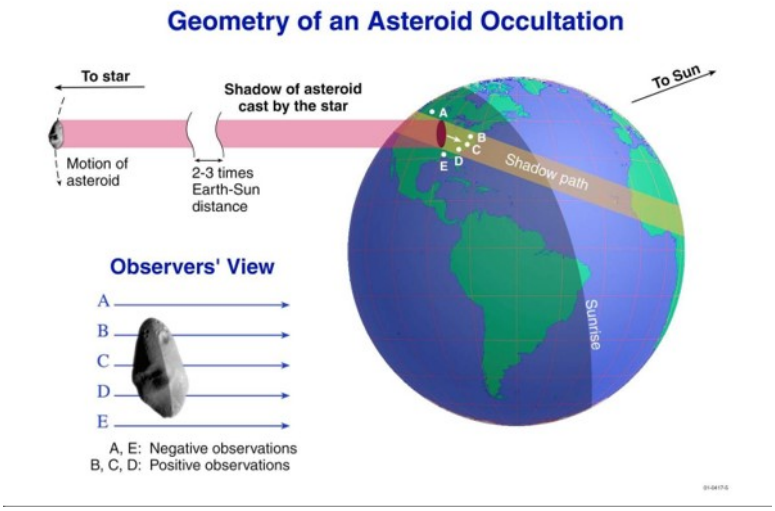

Figure 2.1: Illustration of occultation by a main belt asteroid and path of its shadow on Earth. [1]

Of course, we need some prediction when the occultation happens so that we know which star to observe. This can be done simply with astrometry derived from photometric data. Objects inside our Solar System move on the static stellar background, and we are interested in events when the path of the object intersects the line between Earth and the star.

In that case, the shadow of the objects will display on Earth and will be moving along with the relative motion of the object and Earth. Because the star is much farther from the object, we can suppose that its beams are parallel in the Solar System. Then the shadow on Earth has the same size and shape as a projection of the object.

There are several types of objects that can occult a star. These are moons, planets, and minor planets. For planets, we can get important information about their atmosphere and surroundings. For example, the rings of Uranus (Elliot

[1] `https://occultations.org/occultations/what-is-an-occultation/`

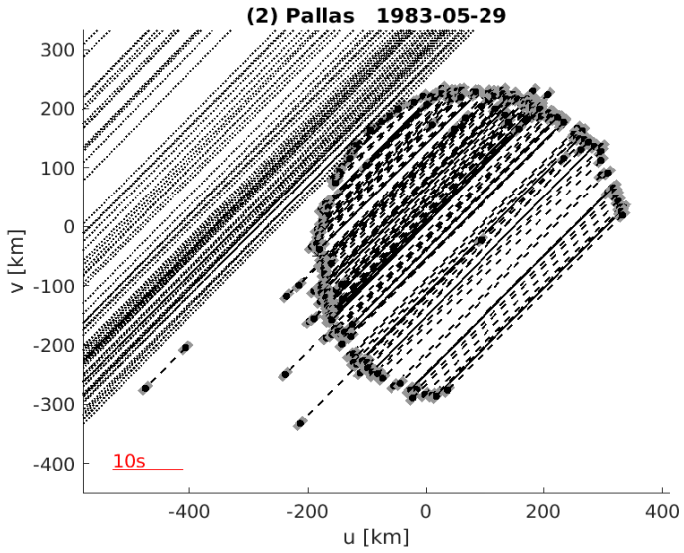

Figure 2.2: Occultation by asteroid Pallas from 1983. Longer dotted lines are negative observations, dashed lines are visual observations, and solid lines are electronically recorded. On the axes are the coordinates at the fundamental plane.

et al., 1978) and the atmosphere of Pluto (Millis et al., 1993) have been discovered using occultations.

The most common observed occultations are stellar occultations by asteroids. It not only allows us to directly observe the shape and size of the asteroid, but observations with only basic equipment have Gaia–level precision in determining the position of the asteroid (see Ferreira et al., 2022). Astrometry for asteroids is usually less precise than for stars because the orbit of an asteroid is determined with higher uncertainty than the almost static position of the star. However, with occultation, we know when the asteroid is observed in the exact same position in the sky as a star. Because if we observe the occultation at a given time, we know that the asteroid is in the same spot in the sky as the star, so we know the asteroid's position with the same precision as that of the star. Therefore, we get the measurement of the position of the asteroid with 0.1 mas precision (see Gaia Collaboration et al., 2021).

Some occultation observations can even detect binary asteroids. When we predict an occultation from a main body, there is a chance that the secondary asteroid will also occult the star. This will show as two disappearances of the star shortly after each other. An example of this is the moon of the minor planet (4337) Arecibo, which was discovered and confirmed by occultations (see Gault et al., 2022) and only after that was confirmed by Gaia.

In addition to collecting useful information about known asteroids, occultations can be used to study populations of minor planets. This is especially useful for smaller TNOs, which cannot be detected using photometry. For asteroids so small and far, we have to consider diffraction during their occultation, which modulates the incoming light from the star instead of just blocking it. Then long-term observations of stars can be made when we look for these diffraction effects. This should give us information about the size distribution of TNOs (see

Roques and Moncuquet, 2000). Even individual kilometer–sized TNOs can be found using this method (see Arimatsu et al., 2019), but they cannot be uniquely identified, because from single occultation we cannot get their orbital parameters.

We can also obtain useful information about the occulted star itself. There are cases when the star is resolved to be a previously unknown binary. An example of this can be the star BD +29 1748 which was occulted by the asteroid (87) Sylvia as presented in Lin et al. (2009).

To work with the observations of occultations, we need to process the data. In order to visualize the observed shadow, we project the observations onto a plane. This is done by projecting the spatial coordinates of the observer in times of disappearance and reappearance of the occulted star to the surface, which is perpendicular to the direction of Earth–Asteroid and co-moving with the asteroid. The precise method of projection will be described in Chapter 3. The final projection is shown in Fig. 2.2.

2.1 History of occultations

The first ever observed occultation was by Mars in 1822. At that time, the astrometry precision was nowhere near enough to predict asteroid occultations. Minor planet occultations have been observed since 1953 when the first occultation by (3) Juno was observed. Since then the number of successfully observed occultations started to increase, especially in recent years; see Fig. 2.3.

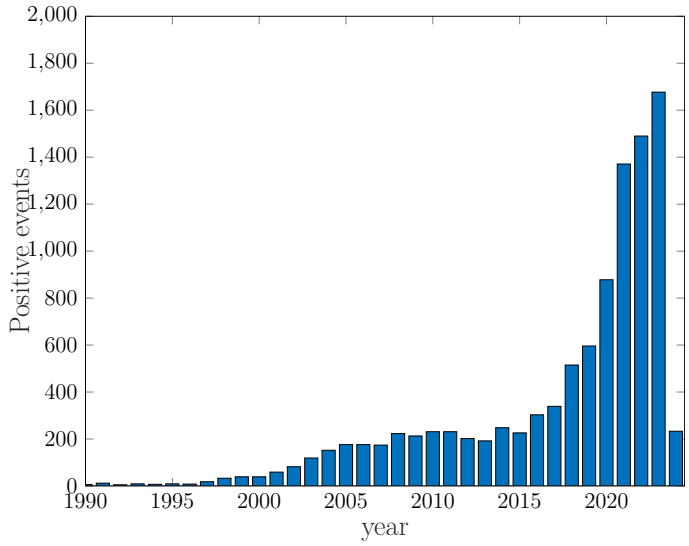

Figure 2.3: Number of positive occultation events in the data set of asteroid occultations, per year. The decrease in 2024 is because I am using data from OccultWatcher[2] from April 2024.

The main reason for the increasing number of successful occultations in recent years is the decreasing uncertainty in astrometry. With more precise positions of asteroids and stars in the sky, we can predict the occultation with higher

[2] `https://www.occultwatcher.net`

accuracy. Observers are then able to position themselves in the path of the shadow more often and that results in more successful observations. In addition, when observers have a higher chance of successful observation, they also have a higher motivation to observe. Another reason for this increase is the availability of observational instruments. This includes telescopes and CCD cameras.

The main influence on the increase of astrometry precision has been recent releases of stellar catalogues. Most important of those are Gaia catalogues (Tanga et al., 2023), which contain both the position of stars and asteroids. Another step forward in the number of successful observations is expected with the Vera Rubin Observatory and its Legacy Survey of Space and Time (LSST) (Ivezić et al., 2019). This survey will not improve astrometry from Gaia, but it should observe many more objects for which occultations could be observed. It could even improve our knowledge to the point where it would be possible to predict the occultations of thousands of TNOs (Camargo et al., 2018).

2.2 Present observations of occultations

To successfully observe the occultation we need our telescope to be in the path of the shadow. And if we want enough information from the occultation, we need to observe it from several positions. Observatories are large, immobile, and too sparse to be efficiently used for occultation observations. This is why we rely on amateur astronomers with small mobile telescopes. They can travel to where the shadow will be, and there are more of them than professional observatories. Because the observation requires precise timing and not as precise photometry (as long as we see the drop in brightness), their observations are sufficient.

With an increasing number of observers and observing events, new organizations have been created to coordinate the observations. Most known among them are:

- International Occultation Timing Association (IOTA)[3]
- International Occultation Timing Association – European Section (IOTA– ES)[4]
- Japanese Occultation Information Network (JOIN)
- Trans Tasman Occultation Alliance (TTOA)[5]

These organizations collect data from observers, evaluate their credibility, and publish them.

There is also the software OccultWatcher[6] which connects observers and provides information for upcoming events. Through it, observers can share their plans for observations and coordinate with each other to cover a whole predicted path of the shadow. (Herald et al., 2020)

[3] `https://occultations.org`
[4] `https://www.iota-es.de`
[5] `https://www.occultations.org.nz/aboutus.htm`
[6] `https://www.occultwatcher.net`

Observers use different methods to record observations, but their results are the same: times of disappearance and reappearance of the star, their uncertainties, and the position of the observer. The most common techniques are as follows:

- Visual observations when the observer uses only the telescope without any recording equipment. Observers observe the star through a telescope by themselves and record the observed time. This method of observation has higher uncertainties (the reaction time of humans is around 0.25 s) but is less demanding on equipment. This method has not been used as often in the last few years because CCD cameras are available to almost everyone.

- Photometric measurements when the output is a light curve of the occulted star or a video of a star field. Uncertainty depends on the exposure time and the readout speed of the used camera, but typically is much less than for visual observation, usually on the order of hundredths of a second. A big advantage is that usually, we can clearly identify the moment of disappearance of the star.

- Drift scan, which is just one image from a CCD camera through a telescope. But in this case, the telescope does not follow the star. There is no movement to match the rotation of the Earth. In that case, each star will not create a point on the image but rather a line. For the occulted star, the line will be interrupted during the occultation. From the position and length of interruption along the line, we can determine the time and duration of the occultation. In this case, the uncertainty depends on the resolution of the picture and the speed of the star in it.

Observers then report their observation as a list of their position, method of observation, and time of beginning and end of occultation (synchronized with GPS) in case of successful observation. Negative observations are also important, especially to limit the size of the asteroid and improve astrometry. In case of bad weather or any other conditions that could compromise the observations, observers can add a note about their observational conditions.

All reported observations are then checked for completeness and correctness before their addition to a database. Completeness requires that all the data mentioned above are reported. The correctness check consists of a comparison with other observers so that their observation is not in contradiction. In addition, these observations are compared to the prediction, and if they differ too much, chances are that the observed events were not the desired occultation. It could, for example, be clouds that covered the observed part of the sky. Even negative events can be incorrect. It could be caused by a too small drop in brightness or that the observer was watching the wrong star. This is especially important in the case of events with one observer (Herald et al., 2020).

3. Using occultations for modelling of asteroids

Occultations can be used in several ways in asteroid modelling. The basic one is to scale a model created from light curves without proper dimensions. Another is solving the pole ambiguity from photometric measurements and inducing non-convexity to asteroid shape models, which are not seen in light curves.

Observations of occultation are available from several sources on the Internet. We use the database of the Occult[1] software, where the data are available in a XML file[2] suitable for further processing.

3.1 Models from photometric measurements

From time-dependent photometric measurements, we can get the asteroid's period, pole position, and shape. But in order to do that, we face an inverse problem. We can directly compute theoretical light curves from the asteroid model, and then we need to find which shape solution fits the observed light curves the best. Asteroid's shape model is given by a 3D object characterized by points in the Cartesian coordinate system and the triangles between these points. This coordinate system is defined by the pole position of the asteroid so that the rotational axis is the z axis. The asteroid revolves around this axis with a period P. The pole position is given by two angles λ and β in ecliptical coordinates. Positions of the x and y axes are given by the initial rotation of the asteroid at one given time.

We can find a convex shape solution only from light curves, which is stable and unique (Kaasalainen and Torppa, 2001; Kaasalainen et al., 2001), but asteroids are not convex bodies. But the non-convexity in asteroids' shapes affects light curves in a way that can be explained by convex shape solutions. So, from light curves alone, we cannot uniquely determine the non-convex model. That is the reason we use mainly imprecise convex modelling from light curves alone. However, the convex solution can be used to find a period and pole position even for a non-convex asteroid.

We will start with determining the period. We are looking for the best-fitting model with the least squares method. But in P, there are many local minima (unlike in shape solution itself with a given period and pole), so we create a periodogram. It consists of creating a few convex models with small resolutions using the least squares method for every given period with different initial pole positions. On the basis of the Root Mean Square (RMS) value of the models, we can find the correct period.

At first, we select the interval in which we estimate our period and then create a set of periods inside this interval. The separation of this periods ΔP is given by

[1] `http://www.lunar-occultations.com/iota/occult4.htm`

[2] `www.lunar-occultations.com/occult4/asteroid_observations.zip`

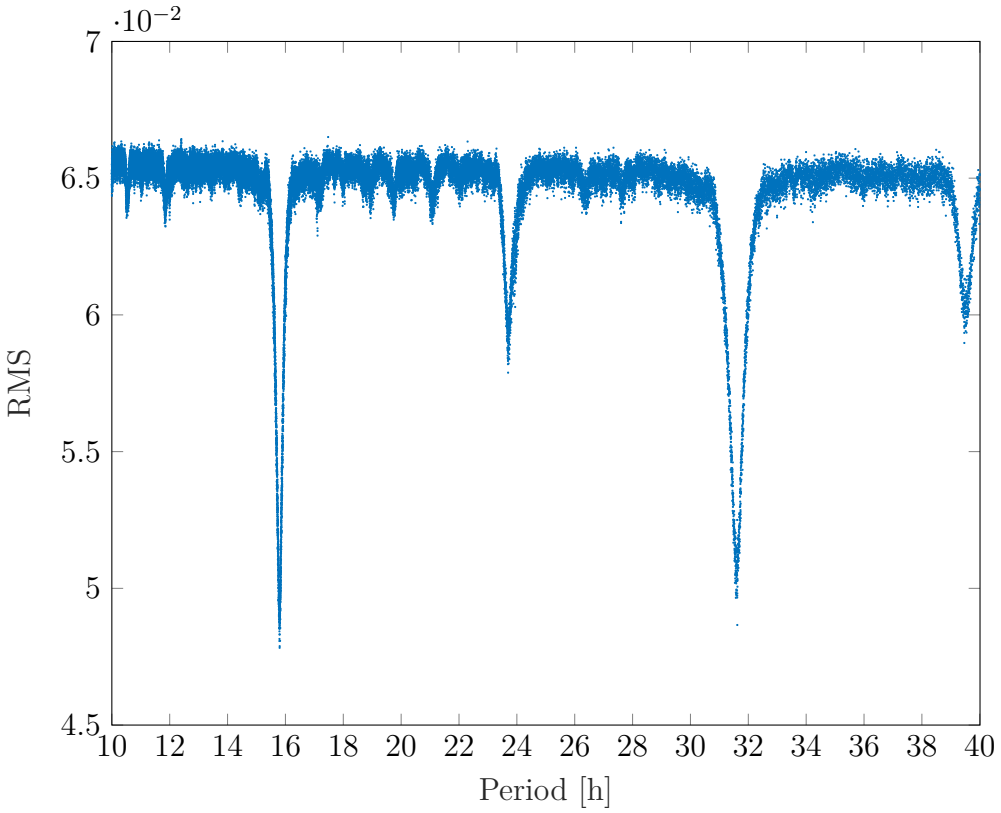

Figure 3.1: Periodogram of asteroid (70) Panopaea. Searched interval is from 10 to 40 hours. Best period is 15.799 h, which has the lowest RMS.

$$\frac{\Delta P}{P} = \frac{P}{2T}, \tag{3.1}$$

where P is the period around which we are computing the separation and T is a time interval covered by observations. This equation tells us how big the change of period must be to shift the light curves for one-half of the period along all observations (see Kaasalainen et al., 2001). So it is an estimate of how far the local minima can be from each other with a given data set. So we make our separation of periods smaller so that we won't miss any local minimum in case it is global. The final value of the period is where the model converges from the initial value. Graphical results of the periodogram can be seen in Fig. 3.1. The determined period is 15.799 h, but several other minima are visible in the periodogram. They are usually at double or half period. That is the reason, why we need our periodogram to cover a big enough interval. We do not want to find only a local minimum.

When we find the period with the lowest RMS, we again create several more models with different initial poles, but this time the pole grid is more dense. Convex modelling has faster conversion in pole, so several initial positions can converge to the same value, yet it does not have to be the global minimum. We then search for the positions with the lowest χ^2. Usually, there are two pole positions with very similar values. They differ approximately by 180° in λ. This ambiguity in the pole position is caused by modelling the 3D shape from planar

observation (see Kaasalainen and Lamberg, 2006). Because observers on Earth are always on the ecliptical plane and in the case when the asteroid's orbit is close to the ecliptic, all observations are in one plane. For that reason,b we usually get two pole positions and for them two models that are mirrored over the observational plane.

3.2 Scaling models

The first step of using occultations in asteroid modelling is to scale existing models. To do that, we need to choose which occultations to use and process their data. We could use all available data, but some occultations are useless for precise model scaling. All occultations with only one or two observers can be fitted to any model only by scaling and shifting. So these occultations are usually used for astrometry determination, but we are not working with them.

To compare the asteroid model and observation of occultation, we need to process observational data. The model is a 3D shape and observations are just positions of observers and time. In order to compare these two, we will project them onto one fundamental plane. The projection for an asteroid is quite straightforward, just a projection of a 3D model onto a plane. But we first need the position of the plane relative to the asteroid and the asteroid's rotational state during occultation.

The fundamental plane is defined as the plane crossing the centre of Earth and is instantaneously perpendicular to the direction from the centre of the asteroid to the occulted star. This gives us two unit vectors which define the fundamental plane

$$\begin{aligned} \mathbf{S}_v &= (-\sin\delta\cos\alpha, -\sin\delta\sin\alpha, \cos\delta), \\ \mathbf{S}_u &= (\sin\alpha, -\cos\alpha, 0), \end{aligned} \tag{3.2}$$

where α and δ are the right ascension and declination of the occulted star. With this, we can project the observer's position at the time of disappearance and reappearance onto the fundamental plane with coordinates

$$(u, v) = (\mathbf{S}_u \cdot (\mathbf{x} + \Delta\mathbf{v}\Delta t), \mathbf{S}_v \cdot (\mathbf{x} + \Delta\mathbf{v}\Delta t)), \tag{3.3}$$

where $\mathbf{x}$ is an observer's position on the Earth in the sidereal equatorial frame. To compute this coordinate transformation from the given position of the observer (longitude, latitude and altitude), we are using JPL Horizons[3]. We also need to know

$$\Delta\mathbf{v} = \mathbf{v}_{Earth} - \mathbf{v}_{asteroid}, \tag{3.4}$$

which is the relative velocity of the asteroid and Earth, which is also taken from JPL horizons. And finally, Δt which is the time difference between the observed event and a chosen epoch (usually the middle of the occultation)(Ďurech et al., 2011).

Now we have the observations projected on the fundamental plane. Each successful observation has one chord with two boundary points. Negative observations consist of a line defined only by the position of the observer. We can take two arbitrary times during the event and get two points on the fundamental

[3] `https://ssd.jpl.nasa.gov/horizons/app.html#/`

plane, which defines the negative chord. The final projection of the occultation is shown in Figure 2.2.

We are working with the assumption that all observations were made around the same time (sufficient usually is within 10 minutes), and the velocity $\Delta\mathbf{v}$ remains constant. Usually, this means that the observations were made on the same continent and Δt is less than ten minutes. Otherwise, we can use a more precise formula instead of (3.3) that includes the change of relative velocity.

$$(u, v) = \left(\mathbf{S}_u \cdot (\mathbf{x} + \Delta\mathbf{v}\Delta t + \frac{1}{2}\Delta\dot{\mathbf{v}}(\Delta t)^2), \mathbf{S}_v \cdot (\mathbf{x} + \Delta\mathbf{v}\Delta t + \frac{1}{2}\Delta\dot{\mathbf{v}}(\Delta t)^2)\right). \quad (3.5)$$

To project the asteroid model onto the fundamental plane, we need to compute its rotational state during the event. Then we need to transform the model from the asteroid's equatorial coordinates $\mathbf{r}_{ast}$ to the equatorial coordinates of Earth $\mathbf{r}_{eq}$.

The first step is to rotate the model around the z axis (rotational axis in equatorial coordinates) by the angle of $\phi_0 + \frac{2\pi}{P}(t - t_0)$, where ϕ_0 is the initial angle at time t_0. Then we rotate the model to ecliptical coordinates. This rotation is given by the position of the pole in ecliptical coordinates (λ, β). And finally, the rotation from the ecliptical coordinates to Earth's equatorial coordinates $\mathbf{r}_{eq}$ by the obliquity of the ecliptic ϵ. We get that

$$\mathbf{r}_{eq} = R_x(\epsilon)R_z(\lambda)R_y(90° - \beta)R_z\left(\Phi_0 + \frac{2\pi}{P}(t - t_0)\right)\mathbf{r}_{ast}. \quad (3.6)$$

Then we project the model onto the fundamental plane similarly to the observations to get the coordinates (u, v) of its silhouette on the plane

$$(u, v) = (\mathbf{S}_u \cdot \mathbf{r}_{eq}, \mathbf{S}_v \cdot \mathbf{r}_{eq}). \quad (3.7)$$

Now we have projected both the observations of occultation and the asteroid's model on the fundamental plane, and we can compare them. We fit them to each other. There are two free parameters we are fitting for each occultation and one joint. These are shifts of the model in the fundamental planes of each occultation and scale of the model, the same for all occultations. The fitted scale then allows us to compute the equivalent diameter of the asteroid. This is the diameter of a sphere that has the same volume as the asteroid. In order to find the right scale and shift, we will use the least squares method, where we will minimize the value

$$\chi^2 = \sum_{j=1}^{N} \frac{\parallel (v_j, u_j)_{occ} - (v_j, u_j)_{model} \parallel^2}{\sigma_j^2}, \quad (3.8)$$

where N is the number of events (both reappearance and disappearance), usually two times the number of observers. Then we have the error of occultation observation σ_j in kilometres, which is computed from time uncertainty simply by multiplying with the asteroid's velocity, and the coordinates of this observation on the fundamental plane $(v_j, u_j)_{occ}$. The coordinates of the model $(v_j, u_j)_{model}$ are harder to determine because we need only one point at the projected silhouette. The point we use lies on the chord of the observation or its extension. Visual illustration of these points is shown in Fig. 3.2. The plot after fitting is visualized in Fig. 3.3.

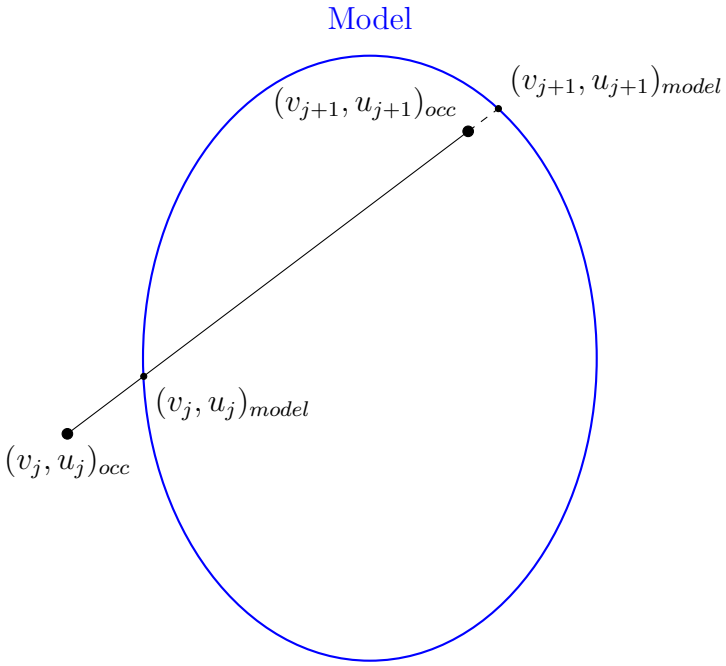

Figure 3.2: Computing of χ^2. The model is ellipsoidal for illustration. The points $(v_*, u_*)_{occ}$ denote ends of chord. The points $(v_*, u_*)_{model}$ denote the edge of the model where it intersects the chord or its extension.

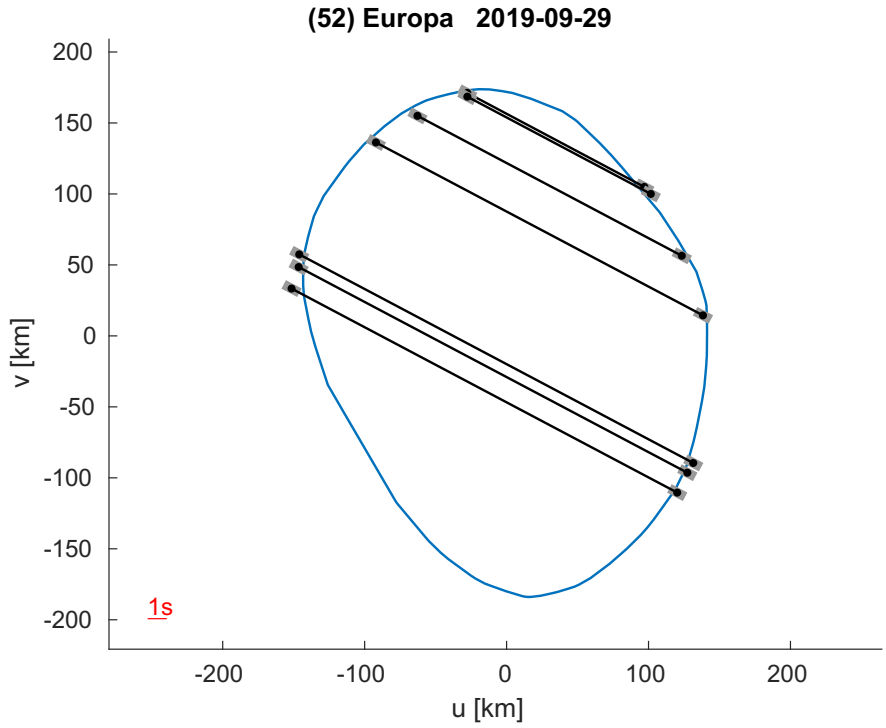

Figure 3.3: Occultation by asteroid (52) Europa from 29 September 2019 with fitted model from DAMIT.

Now we need to find asteroids for which to scale their models. We will use all asteroids that have a model in DAMIT and at least one occultation with at least four positive observations. For all of these asteroids, we will fit and plot their occultations to their models. Based on these plots we are then able to determine whether the model corresponds with occultations observation or not. This is done by visual comparison. There is of course the value χ^2 from the fitting, and then we can compute the RMS value, but both can be misleading. In cases when an asteroid's pole position is ambiguous and therefore has more models in DAMIT, we are even capable of determining which of the two models is better. Models from light curves are ambiguous, but occultations are not, and if we have one densely enough observed with the correct rotation of the asteroid, we are able to choose between models (see Fig. 3.4).

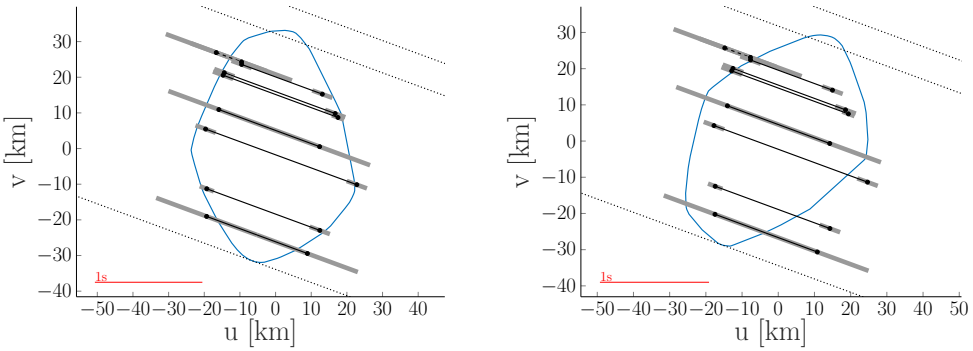

Figure 3.4: Occultation by asteroid (64) Angelina from 3 July 2004 with two fitted models from DAMIT. The first model (left) agrees with the occultation, while the other one does not.

In some cases, we cannot distinguish between the two models of asteroids, because they have a very similar projection at the time of occultation. Several asteroids already have only one model in DAMIT and in that case, we can only say whether observed occultations correspond to this model or not. Asteroids with no corresponding model are now our primary candidates for new model creation.

3.3 New model creation

If we find an asteroid with a model that does not agree with observed occultation, we need to improve the model. Even if we know that the model is not correct, we can't say whether only the shape solution is not correct or also the period and pole position. It might be enough to improve the shape solution for the model to fit the data. Period and pole position could still be right. But sometimes even the pole position and period could be incorrect. In both cases, we need to create a new model using both light curves and occultations and find possible periods and pole positions from light curves. Convex occultations use different representations of shape models, such that allow fast optimization but do not allow computing a projection for occultation fitting. So in order to use occultations in model creation we need different shape representations. This also allows us to add non-convexity

in model creation. This could give us unique non-convex models of asteroids, that fit non-convex features in occultations, such as is shown in Fig. 3.5. For this, we need more densely covered observations of occultations than for just model scaling and fitting. We will work only with asteroids that have at least one occultation with ten or more chords. This gives us a large enough set of asteroids, even when we include a criterion for no or non-corresponding model in DAMIT.

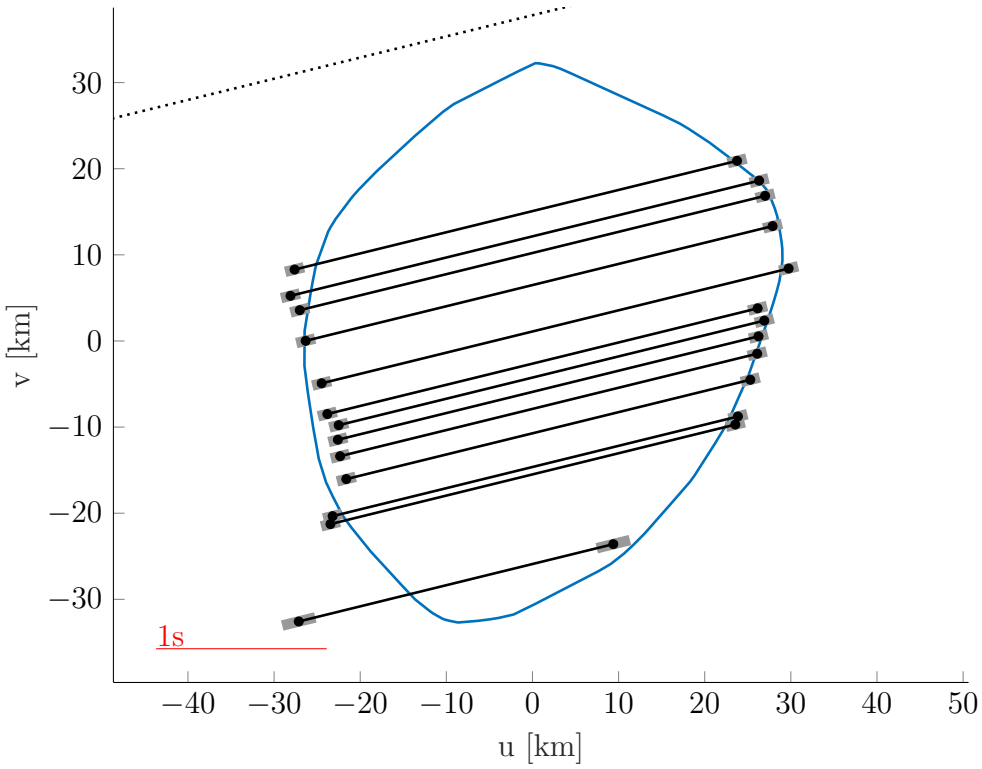

Figure 3.5: Occultation by asteroid (258) Tyche from 8 October 2022, with distinct non-convex feature on the left side, and convex model from DAMIT. The convex model corresponds only partially with the occultation, as it is convex and the occultation is non-convex.

After this selection, we are left with 37 asteroids, for which we will try to create a new model. But first, we will need to create a dataset of light curves and occultations to use.

In this work, I use photometric data stored by my supervisor Josef Ďurech and Josef Hanuš. Most of these data are dense light curves obtained by short-term observation of asteroids. The data usually covers the time of several hours with hundreds of measured values. Most of the data can also be obtained from the Asteroid Lightcurve Data Exchange Format (ALCDEF)[4] database (Warner et al., 2011). I also use sparse data from Gaia, The Asteroid Terrestrial-impact Last Alert System (ATLAS) and All Sky Automated Survey for Supernovae (ASASSN). Gaia is a spacecraft primarily designed for stellar astrometry and photometry (Gaia Collaboration et al., 2016). But it also records the asteroids' position and brightness in the field of view with higher precision than most Earth-bound observations

[4] `https://alcdef.org`

(Mignard et al., 2008). ATLAS is a NASA system for early warning of asteroid impact. It consists of four telescopes which scan the whole sky several times each night (Tonry, 2011). And ASASSN is an automated survey designed to search for supernovae (Dong et al., 2016). The sparse light curves cover a much larger time span. It could be as large as several years and measurements are with much smaller frequency than with dense light curves. Instead of several values per hour, we have only several values per month. For most asteroids, this gives us several dozens of light curves (both sparse and dense), which is enough to find the correct period and candidates for pole position (even if ambiguous).

After the selection of asteroids, we will use all occultations with more than three successful observers. Occultations with fewer chords usually make little difference in model creation, but can in principle be used. Even if only for later model verification.

For our model creation, we will use the All-Data Asteroid Modelling (ADAM) software (Viikinkoski et al., 2015). This algorithm uses optimization methods to solve an inverse problem from observed data.

The shape representation in ADAM can be of two types. One, an octantoid, uses spherical harmonics to describe shapes, and the parameters of these functions are used in minimization. The other representation is the subdivision surface, where the shape is described by a set of vertices and corresponding triangles. The minimization parameters for this case are the position of the vertices.

We are mostly using the octantoid representation, which is given by a vector $p \in R^3$ and its parametrization is

$$p(\theta,\varphi) = \begin{cases} x(\theta,\varphi) = \exp\left[a(\theta,\varphi)\right]\sin\theta\cos\varphi, \\ y(\theta,\varphi) = \exp\left[a(\theta,\varphi)+b(\theta,\varphi)\right]\cos\theta\cos\varphi, \\ z(\theta,\varphi) = \exp\left[a(\theta,\varphi)+c(\theta,\varphi)\right]\cos\theta, \end{cases} \tag{3.9}$$

where a, b, c are linear combinations of the spherical harmonic functions $Y_l^m(\theta,\varphi)$ with coefficients a_{lm}, b_{lm}, c_{lm} and x, y, z are coordinates in the Cartesian system. Several regularisation terms are used that help to conserve the shape model physical. It is assumed that the basic asteroid shape is geometrically starlike, which means that each radius vector crosses the surface only once. The term

$$\eta = \sum_{l,m} l(b_{lm}^2 + c_{lm}^2), \tag{3.10}$$

is added to the minimization in order to keep the model starlike. It adds a penalty to the χ^2 term for any deviation from the starlike shape and pushes the solution toward this shape.

Apart from the regular shape, it is also undesirable for the dihedral angles to be too sharp. Therefore, we add regularization that keeps adjacent facets parallel. To do this, the direction of facets normal vectors is used. The regularization is then

$$\gamma = \frac{1}{\sum_j A_j}\sum_{i,j} A_j(1 - \mathbf{v}_i \cdot \mathbf{v}_j), \tag{3.11}$$

where A_j is the surface of a facet j and $\mathbf{v}$ its normal vector. Summations over j are only over facets that are adjacent to the facet i.

The optimization itself contains terms which express the fit of light curves and occultations to the model. The term for occultations is similar to that in Equation (3.8)

$$\chi^2_{occ} = \sum_{j=1}^{N} w_j \left[(v_j, u_j)_{occ} - (v_j, u_j)_{model}\right]^2, \tag{3.12}$$

where w_j is the weight of individual chords, usually set to one. This holds for positive chords. But for negative chords points $(v_j, u_j)_{occ}$ do not exist, so the penalty term is added to the χ^2_{occ} if the negative chord intersects the model. Similarly, we add a different penalty when a positive chord does not intersect the model. In that case, the added penalty is based on the distance of the chord from the model.

A term for light curve fit is simpler when we only compare the model and measured intensity at a certain point in time. This is done for all measurements:

$$\chi^2_{LC} = \sum_{i=1}^{M} w_i (I_{measured} - I_{model})^2, \tag{3.13}$$

where the sum is over all points from all light curves. The term I_{model} is the integrated relative brightness of the asteroid that depends on the shape, observational geometry, and albedo of the asteroid. As for the albedo, which we do not know, it is usually assumed to be constant over the asteroid's surface and we work with relative light curves, so we need not know its value. Here the weight w_i of individual light curves is chosen as one for all dense light curves. It is less for most sparse light curves because data from ASAS and ATLAS are not as precise since their primary focus is not the photometry of asteroids. On the other hand, sparse light curves from Gaia have higher precision as it is focused on photometry, so I gave them higher weight.

The final value which we minimize is the combination of all the previous terms

$$\chi^2 = \lambda_{occ}\chi^2_{occ} + \lambda_{LC}\chi^2_{LC} + \sum_l \lambda_l \gamma_l^2, \tag{3.14}$$

where λ_* is a chosen weight of individual terms and l goes over all regularization terms. Free parameters are offsets of occultations, shape model parameters, and spin (period and pole position). The minimization of χ^2 is then done using the Levenberg–Marquardt algorithm. For a more detailed description and other data processing in ADAM see Viikinkoski et al. (2015).

By means of this optimization, we can create new models using both occultations and light curves. These models show non-convex features of asteroids and have precise dimensions.

4. New models

Both have some chords that obviously disagree with the oIn this work I processed all available data of occultation observation and used them to improve our knowledge about asteroids' shape and size. There are more than 16,000 models in DAMIT belonging to over 10,000 asteroids. In my bachelor thesis (Černý, 2022) I have performed scaling of models for 274 asteroid, chosen for their observed occultations. For them, I have processed 516 observed occultations. Most of these asteroids (190) have a model in DAMIT that agrees with occultations and I have been able to successfully find its dimension. Another 44 asteroids had a model which I was not able to fit on occultations and 40 had unusable occultations. These asteroids that have non-fitting models are my primary subject in further study and new model creation.

Then I created new models for asteroids that had no model so far or their model did not correspond with the occultation. At first, I created a list of all asteroids that have at least one occultation with at least ten observers. From them, I have excluded asteroids that already have scaled models from my previous work. For the rest, I have created a data set of light curves and occultations. This group contains both the asteroids whose model I was not able to fit on occultations and asteroids that have no model in DAMIT, even though we have enough data about them. I used light curves alone to create a periodogram and determine the period and pole position of asteroids. Then I used these values as initial parameters in ADAM along with all data and created a new model with the proper parameter settings. These settings could differ according to the size of our data set and the need for regularization.

The parameters in ADAM are the weights of individual terms as seen in Equation (3.12). It was necessary to find a balance between the fitting of the data and keeping the shape physical. This varies between individual asteroids due to the different amounts of data and their credibility. As can be seen in Fig. 4.1 and in Fig. 4.3, ADAM can fit the model to the data in more than one way, but some shapes are less physical, as shown in Fig. 4.2. We can see, that both these models fit the occultations quite precisely, but not light curves. The RMS value of light curves fit is almost the same for both of these models, so we still cannot distinguish between them. I also have the initial convex model, which fits light curves slightly better, but has a worse fit to the occultation. And because the occultation has some clear non-convex features, I did not consider the convex model to be correct. We still cannot distinguish between the non-convex models based on data alone and in addition, the photometric and occultation data do not support the same model. But we were at least capable of solving the pole ambiguity. From light curves alone I got five possible pole positions. This suggests that the light curves are not enough to choose a correct model. After the creation of the shape solution with occultation, one pole position had a much better fit to both occultation and light curves than any other. So we can consider this pole to be the correct one and select from its shapes solutions that fit the data the one that has a simpler shape.

I have also checked all the data for correctness. In the case of occultations, this consists of projecting the event and comparing the chords. This way, I can

exclude observers that obviously do not fit the others. An example can be seen in Fig. 4.4 where there are two occultations of the asteroid (423) Diotima. thers. There are several possibilities as, to why chords do not have to correspond to each other. Among them are double stars and binary asteroids, which can cause multiple events during one observation, and false positive observations, when the observed disappearance of the star is not caused by asteroid occultations. Based on a commentary from observers, we can conclude that these observations are indeed wrong and not a double event. Some of these false positives are caused by clouds passing in the field of view and recorded as stellar disappearance. However, because of them, the fitting of a convex model cannot be done properly, just as the modelling itself. So, I excluded these chords and did not work with them further. Also, observations of moons and double events in the case of binary stars are not desirable. The small secondary body can be excluded from occultation (the large body has a strong influence on the light curves, which makes modelling impossible). Also, observations of binary star occultations can be split into two events if the observations are precise enough to distinguish a double brightness drop.

But before I can work with occultations, I need to process the data. The data is available as an XML file, and the processing for the occultation projection is mathematically described in Chapter 3. For this process, I am using a set of scripts written and implemented in Matlab, which I have modified to work with JPL Horizons, where astrometry of the asteroid and coordinate transformation are obtained. This consists of reading an XML file, finding all the occultations of a desirable asteroid, loading information about the observations, and then projecting it onto the fundamental plane. But even when I have the data in the desired format to model fitting, I still need to convert them into a format suitable for ADAM. This consists of simply writing the correct values in a given order and connecting all occultations in one file.

For light curves, I did not have to do any processing but still had to check them for correctness. I even deleted whole observations, in case a convex model fits several dozens of other light curves, as shown in Fig. 4.5. In addition, these light curves often show some weird features, which are probably caused by wrong observations.

This way I processed 34 asteroids. I worked with asteroids that have various sizes of photometric data sets. The largest ones contain over a hundred light curves, whereas some have only about a dozen. A complete list of data set sizes and asteroids with which I worked can be found in Table 4.1. For every one of these asteroids, I made a periodogram, found possible pole positions, and for each created a shape model.

I divided these asteroids into groups based on their new and old models. The first group are asteroids that already had a convex model in DAMIT, but I was able to create a better convex model. The second group are asteroids without a previous model in DAMIT but with a new convex model. The third, most interesting group, are asteroids whose new model is non-convex. They could have a previous convex model from light curves, but occultations show non-convex features, or they did not have any previous model at all.

I have also computed the equivalent diameter for each asteroid and its interval of uncertainty. This interval is based on two more models of each asteroid with

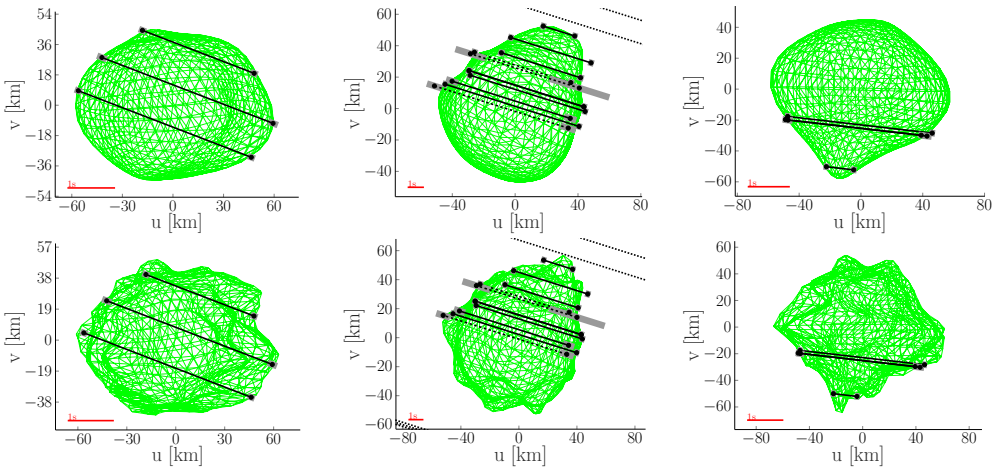

Figure 4.1: Two models of asteroid (788) Hohensteina from ADAM with same pole position, fitted to three occultations. Both models have similar fit to the data, but the second one (bottom) has unrealistic shape.

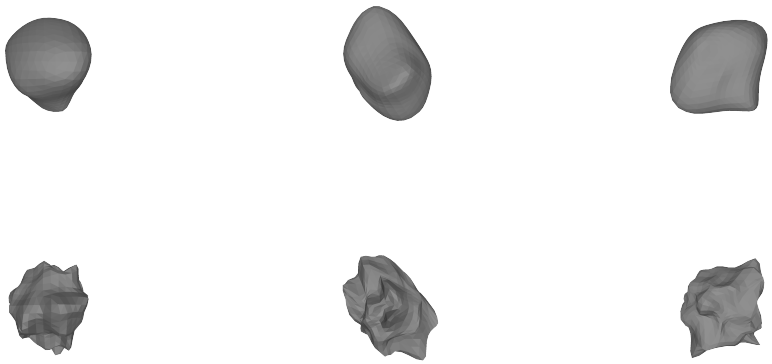

Figure 4.2: Visualization of two models of asteroid (788) Hohensteina from ADAM with same pole position. The second model has unrealistic shape.

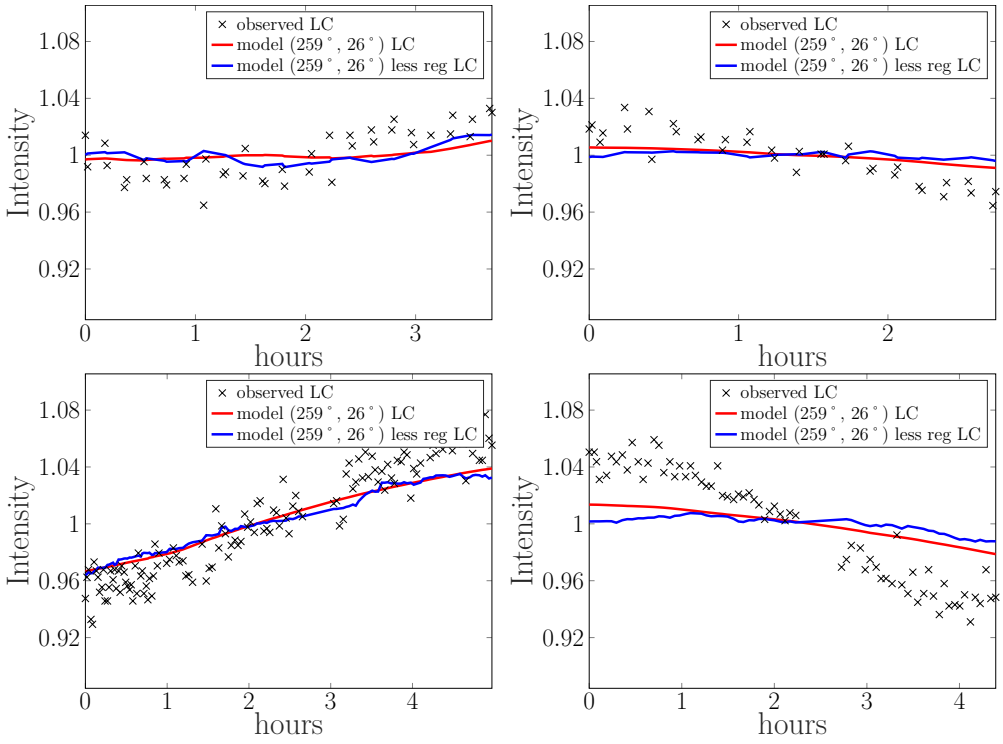

Figure 4.3: Two models of asteroid (788) Hohensteina from ADAM with same pole position, fitted to four light curves. Both models have similar fit to the data, none of them fits perfectly.

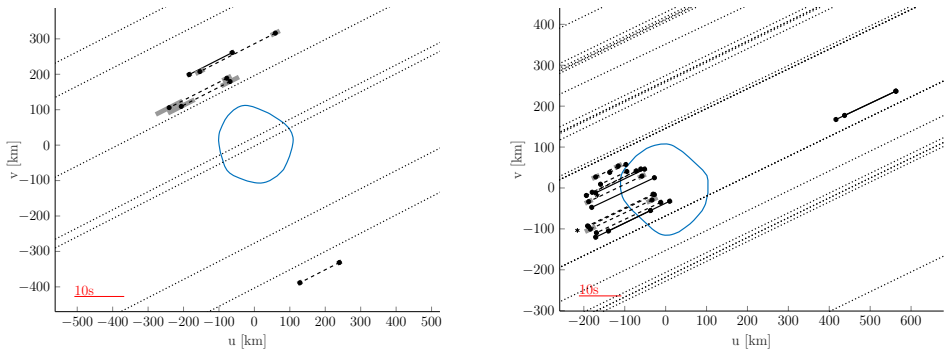

Figure 4.4: Two occultations of the asteroid (423) Diotima. We can see one obviously wrong chord in the first occultation and two in the second.

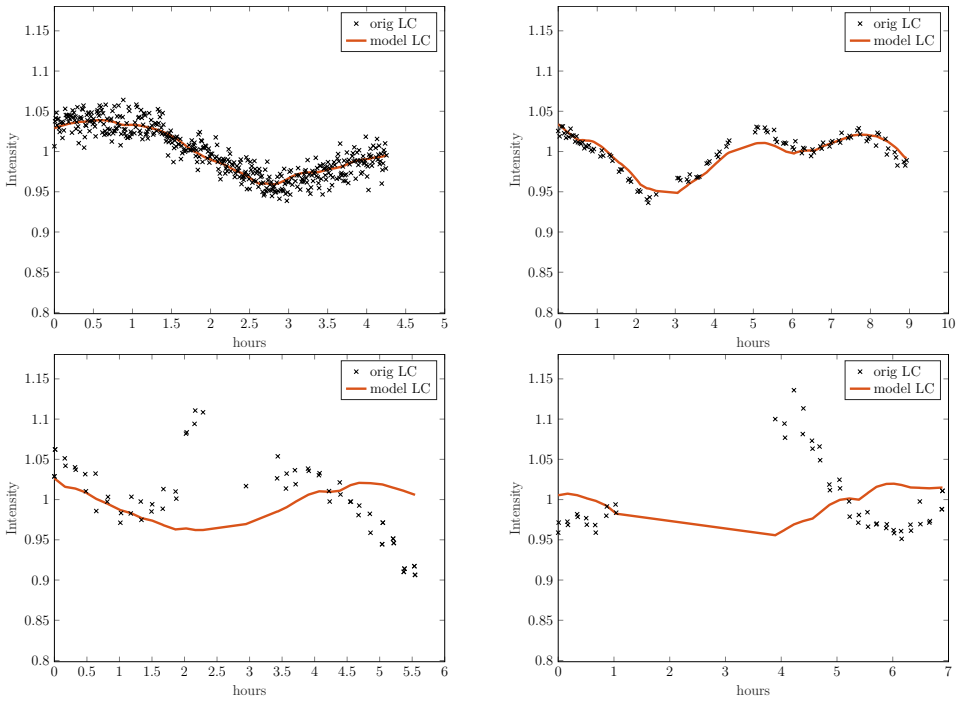

Figure 4.5: Four light curves of asteroid (702) Alauda. The first two light curves are examples of how most of them fit the model. The other two are poorly measured data that do not fit the model and show some unexpected features. Therefore they were later removed from data set.

different input data. The change in data consists of extending and shortening all the occultation chords by their observational uncertainty. This way I got two new models, one larger and one smaller than the original one. Each chord has different uncertainty, so each shape is a little different and after computing the equivalent diameter for each of them, I get an estimate of an interval of the possible diameters. These values are given in tables 4.2, 4.3, and 4.4 as indexes of diameter values. But if we want to know the standard deviation of an asteroid's diameter, I created 50 more models for several asteroids. For each model, I have changed the time of occultation observations randomly according to their uncertainty and normal distribution. This allowed me to find the distribution of possible diameter values and determine its mean value and standard deviation. There are more ways of changing the input (like changing light curves data set, regularization, data weights...) to get a different model with different diameters. However, there are too many possibilities to do it for all asteroids. So I only changed the observations of occultations, because based on them the diameter is determined. Light curves are relative and determine only the shape of asteroids and regularization determines how the model is created. The value of standard deviation σ is also given in table 4.2, 4.3, and 4.4. I give both types of uncertainty, in order to demonstrate the extreme cases of models and their standard deviation differences.

The correlation between my derived diameter from occultation modelling and diameter derived from IR observation can be seen in Fig. 4.6. Diameters from IR are taken from NEOWISE measurements (Mainzer et al., 2019). Larger uncer-

tainty from occultation suggests that even the model itself has higher uncertainty. This is usually because of larger observational errors or bad distribution of chords. If all chords are at one part of the model, even small changes in their length can cause large changes in other parts of the model. Most asteroids have similar equivalent diameters from both IR and occultations or at least within their uncertainty. Usually precision from IR measurements is better for most asteroids, but there are still a few asteroids for which diameter from occultations is more precise. So there is an improvement of asteroids' diameters from occultations. For several asteroids, their diameters do not correspond with each other. Three of them are asteroids (106) Dione, (153) Hilda, and (451) Patientia that have smaller diameters from occultations than from IR. But even though the uncertainty is in this case larger for occultations than from IR, modelling from occultations does not allow for larger dimensions. So I would expect that the uncertainty of diameter from IR measurements is underestimated in these cases. For asteroid (78) Diana I can conclude that the diameter from occultations is better based on uncertainty, which is smaller and the value lies inside the possible interval of diameter from IR.

4.1 Asteroids with improves convex models

At first, I will focus on the group of asteroids that already had an existing model in DAMIT, but it did not correspond to observed occultations, and their new model from ADAM does not have non-convex features. There are seven asteroids in this group, as can be seen in Table 4.2. All of these asteroids have only one final position of pole, which fits best both occultations and light curves. There can also be seen asteroid's final pole position, equivalent diameter from both occultation modelling and IR observations.

4.1.1 (134) Sophrosyne

An example of this group is the asteroid (134) Sophrosyne. It had two previous models in DAMIT, both convex. We can see their projections of occultation in Fig. 4.7. There are visible discrepancies between models and occultations, especially with the first occultation, but neither the second one agrees sufficiently well. Even though the fit on the second occultation is good enough to give us some approximate scaling of the model, we can say that these models are probably incorrect.

The data set of (134) Sophrosyne contains seventeen light curves and two occultations. From the light curves only I have created a periodogram and determined the period at 17.19 h. For this period, I found two possible pole positions: $(100°, 43°)$ and $(280°, 39°)$ and created a shape model for both of them with ADAM. Projection of these models to occultations can be seen in Fig. 4.8. There we can see that the first model fits better to both occultations than models from DAMIT, whereas the second model fits worse. The fact that the first model is better can also be seen in light curve fitting, where the RMS for the first model is 0.032 and for the second 0.056. The graphical fitting of light curves can be seen in Fig. 4.9. Therefore, I have determined that the initial pole position $(100°, 43°)$ from convex modelling is the correct one. For this initial pole position, non-convex

Table 4.1: List of asteroids and their data sets, including number of light curves (lc), number of occultations (occ), found period and number of possible pole positions from light curves.

	Asteroid	lc	occ	period [h]	poles
(50)	Virginia	53	3	14.31	3
(55)	Pandora	38	2	4.80	3
(70)	Panopaea	24	1	15.80	4
(78)	Diana	17	3	7.29	3
(81)	Terpsichore	23	2	10.95	3
(105)	Artemis	60	6	37.12	2
(106)	Dione	12	5	16.21	3
(115)	Thyra	41	2	7.24	2
(134)	Sophrosyne	17	2	17.19	3
(135)	Hertha	46	2	8.40	3
(138)	Tolosa	5	1	10.10	3
(145)	Adeona	45	2	15.07	9
(153)	Hilda	44	6	5.96	3
(200)	Dynamene	25	1	37.40	3
(205)	Martha	32	1	14.90	3
(258)	Tyche	14	3	10.04	2
(275)	Sapientia	36	9	14.93	3
(308)	Polyxo	14	5	12.03	3
(363)	Padua	10	1	8.40	3
(372)	Palma	42	7	8.58	2
(375)	Ursula	34	6	16.90	3
(411)	Xanthe	16	1	7.20	3
(420)	Bertholda	7	6	10.99	3
(423)	Diotima	62	10	4.78	3
(424)	Gratia	15	3	20.06	3
(451)	Patientia	134	8	9.73	9
(506)	Marion	22	1	13.55	3
(521)	Brixia	33	5	28.49	9
(554)	Peraga	52	8	13.71	3
(624)	Hektor	99	7	6.92	3
(702)	Alauda	142	7	16.70	3
(712)	Boliviana	13	4	23.46	2
(788)	Hohensteina	32	3	37.18	3
(914)	Palisana	13	3	8.68	3

Table 4.2: List of asteroids with better convex models with their pole position and equivalent diameter from occultations and IR. . There are two types of uncertainty for equivalent diameter one is extremal interval based on possible biggest and smallest model and σ is stndard deviation based on 50 created models.

Asteroid		pole position	D [km]	σ [km]	D_{IR} [km]	$\sigma_{D_{IR}}$ [km]
(50)	Virginia	(303°, 51°)	$85.6^{+1.5}_{-1.1}$	0.6	84.1	0.2
(106)	Dione	(238°, 28°)	$173.9^{+10.4}_{-16.0}$	15.1	207.9	2.2
(134)	Sophrosyne	(100°, 43°)	$104.1^{+2.5}_{-2.0}$	1.5	104.5	1.3
(372)	Palma	(50°, 54°)	$184.7^{+12.6}_{-6.5}$	3.7	173.6	2.8
(424)	Gratia	(351°, −24°)	$72.5^{+0.5}_{-1.3}$	3.0	102.6	0.6
(624)	Hektor	(334°, −29°)	$182.3^{+3.1}_{-8.4}$	7.4	147.4	2.3
(712)	Boliviana	(87°, 36°)	$121.5^{+5.2}_{-9.4}$	3.0	124.1	1.3

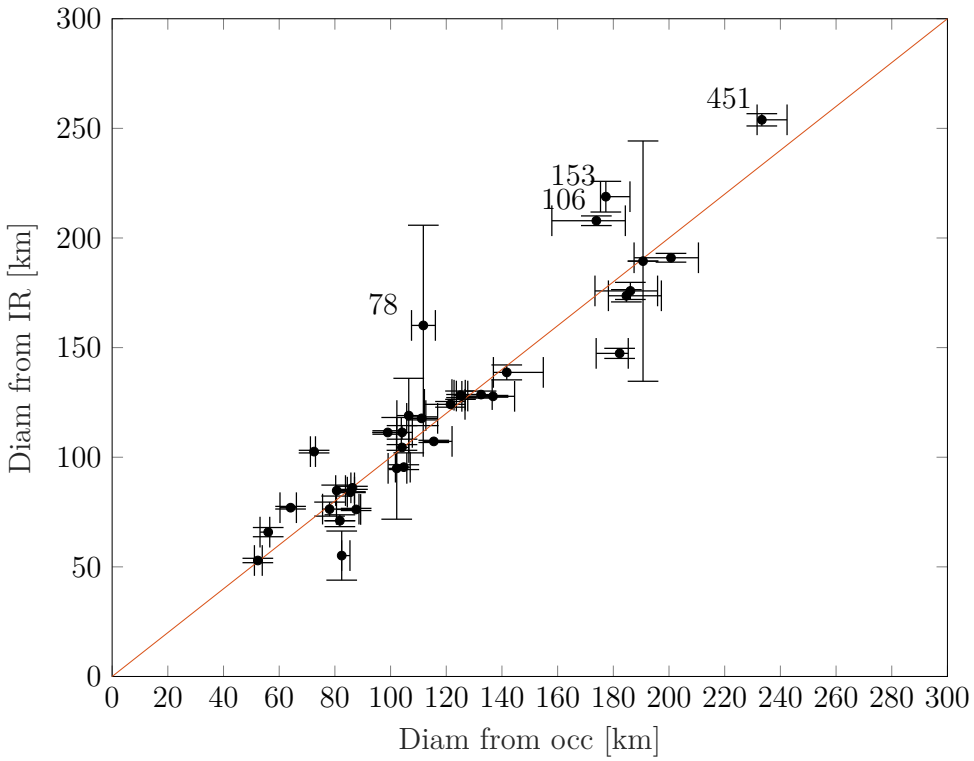

Figure 4.6: Correlation between diameter derived from occultation modeling and from IR measurements with linear line plotted where diameters are equal. Denoted are identification numbers of asteroids far from linear plot.

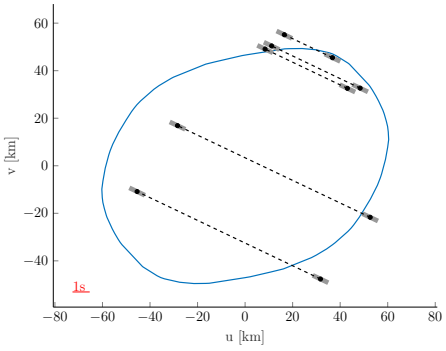

(a) Model 5976 with first occultation

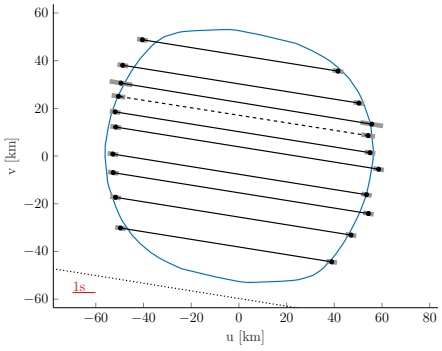

(b) Model 5976 with second occultation

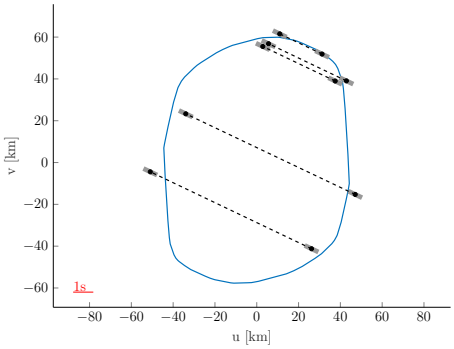

(c) Model 5977 with first occultation

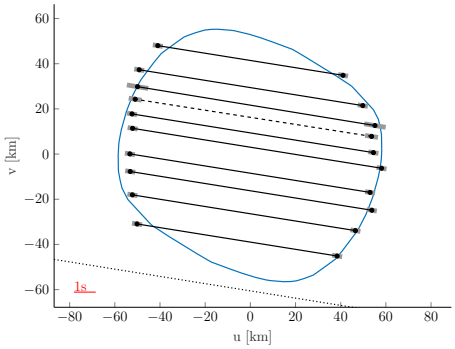

(d) Model 5977 with second occultation

Figure 4.7: Two models of asteroid (134) Sophrosyne from DAMIT, fitted to two occultations from 24 November 1980 and 26 November 2013. Neither of these models correspond with the occultations.

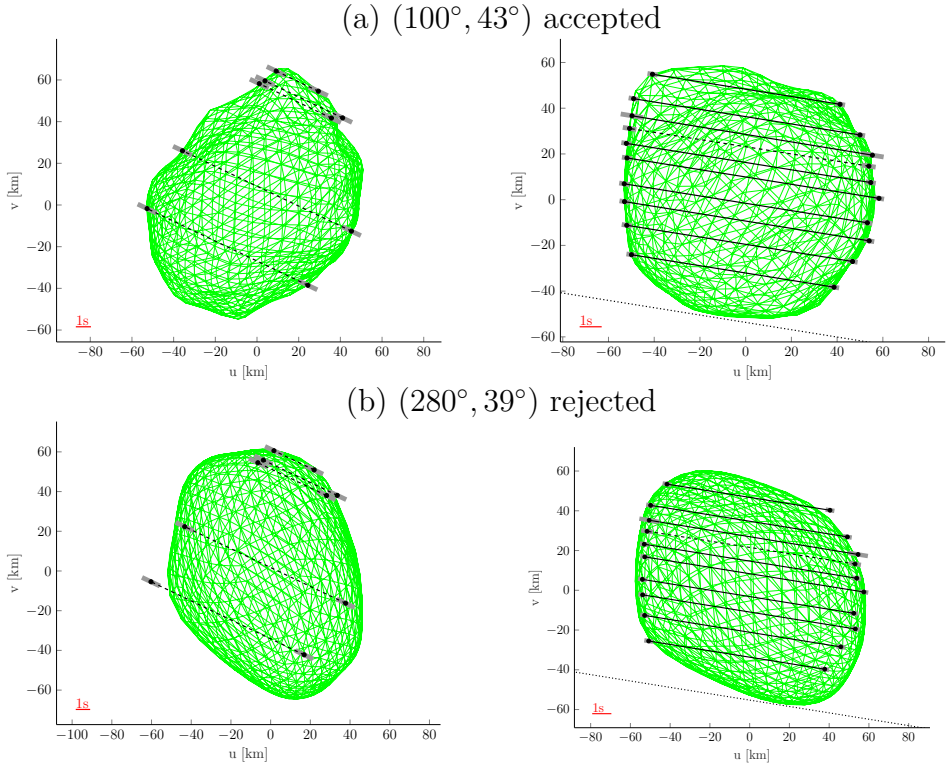

Figure 4.8: Two models of asteroid (134) Sophrosyne created from ADAM, which are identified by their pole position, fitted to two occultations from 24 November 1980 and 26 November 2013.

modelling with ADAM converges to the value $(100°, 35°)$, which is the same as one model in DAMIT. Also, the period I found is the same. So the model from DAMIT had correct parameters, only the shape solution was not precise.

4.2 Asteroids with new convex models

The second group of asteroids consists of asteroids that had no previous model in DAMIT, and their new models from ADAM have no non-convex features. There are seven of these asteroids. They are listed in Table 4.3. Not all of these asteroids have only one final position of the pole. Asteroids (451) Patientia and(702) Alauda have two possible pole positions because the models have a very similar fit to the data.

4.2.1 (81) Terpsichore

For asteroid (81) Terpsichore, there are 18 dense light curves available and two observed occultations. Light curves gave me a period of 10.95 h and three possible pole positions. I will now present the two best models with pole positions $(25°, 0°)$ and $(203°, -8°)$. After finding their shape and fit to both occultations and light curves, I was able to determine, that the model with pole position $(203°, -8°)$. This could be especially seen from light curves in Fig. 4.11 with the RMS values

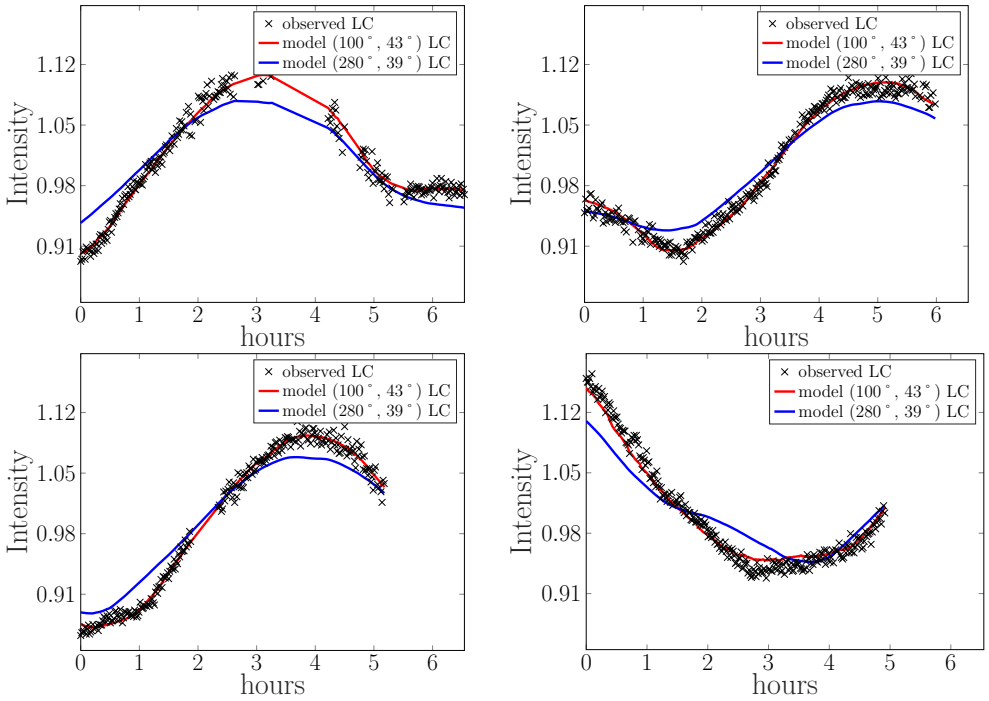

Figure 4.9: Four exemplar light curves of asteroid (134) Sophrosyne with two models' fits. The model $(100°, 43°)$ fits the data better than the model $(280°, 39°)$.

Table 4.3: List of asteroids with new convex models with their pole position and equivalent diameter from occultations and from IR. . There are two types of uncertainty for equivalent diameter one is extremal interval based on possible biggest and smallest model and σ is stndard deviation based on 50 created models.

Asteroid		pole position	D [km]	σ [km]	D_{IR} [km]	$\sigma_{D_{IR}}$ [km]
(81)	Terpsichore	$(203°, -8°)$	$111.2^{+5.7}_{-5.4}$	1.8	117.7	0.7
(145)	Adeona	$(102°, 40°)$	$136.8^{+7.8}_{-11.2}$	1.7	127.8	0.4
(308)	Polyxo	$(295°, 36°)$	$132.5^{+4.0}_{-10.5}$	2.2	128.6	1.6
(420)	Bertholda	$(262°, 80°)$	$141.7^{+13.1}_{-4.8}$	1.8	138.7	3.4
(451)	Patientia	$(175°, 45°), (353°, 5°)$	$233.3^{+9.1}_{-1.7}$	1.3	253.9	2.8
(702)	Alauda	$(334°, -46°), (85°, -59°)$	$200.7^{+9.9}_{-13.3}$	2.1	191.0	2.0
(914)	Palisana	$(209°, -20°)$	$87.6^{+1.6}_{-7.1}$	5.9	76.2	0.5

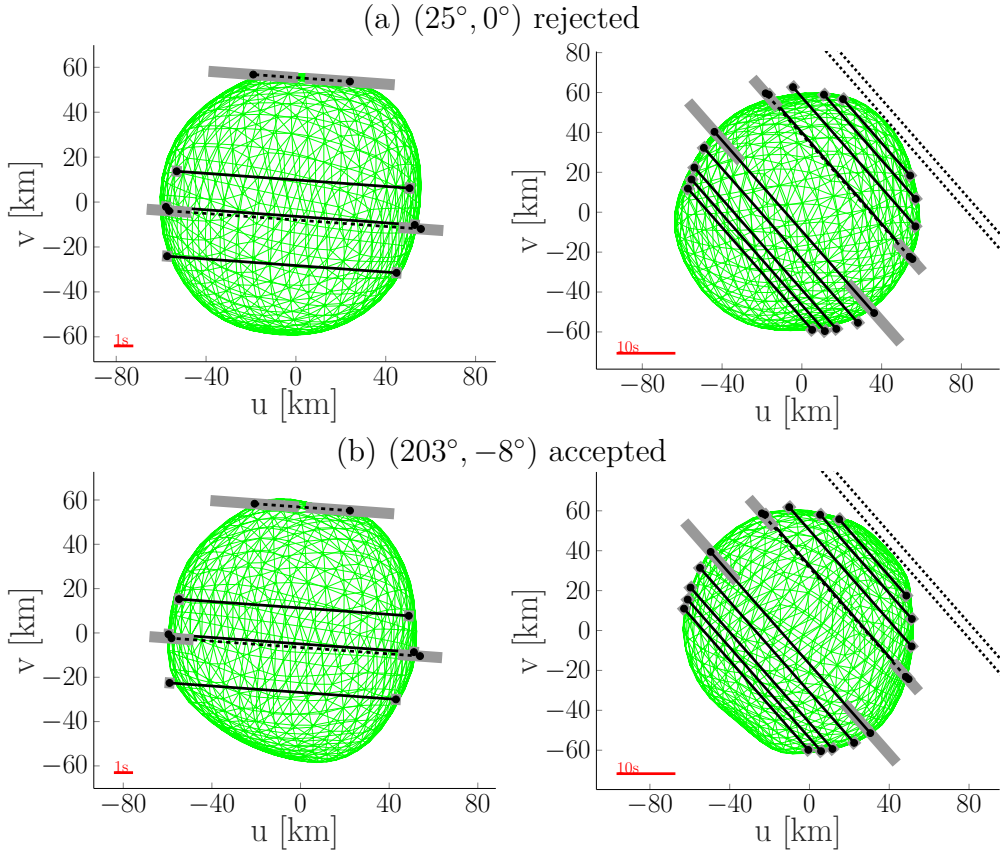

Figure 4.10: Two models of asteroid (81) Terpsichore from ADAM with projections to two occultations.

0.029 vs 0.036. The occultations fit is similar for both models as can be seen in Fig. 4.10. The final pole position for the better model is (206°, −9°).

4.2.2 (145) Adeona

Asteroid (145) Adeona has a data set containing 41 dense light curves and two occultations. Unfortunately, this still gives me eight possible pole positions from light curves with a period of 15.07 h. But with the occultation modeling, I was able to identify the one best pole position. In Fig. 4.12 we can see the fit to occultations for the two best models with pole positions (102°, 40°) and (287°, 4°). Clearly, the model with pole (102°, 40°) is better, which is also seen from light curves fit in Fig. 4.13 and its RMS value 0.015 vs 0.043. The final pole position after shape creation is (101°, 50°).

4.2.3 (308) Polyxo

This asteroid has only nine dense light curves, but five occultations. Even from this small data set of light curves I determined the period to be 12.03 h and with it two possible pole positions. They are (111°, 27°) and (295°, 36°). I created a shape model for both of them and managed to chose the correct one, (295°, 36°). This is based on the fit to the occultations in Fig. 4.14, because both models have a very similar fit to the light curves which is shown in Fig. 4.15. The final pole

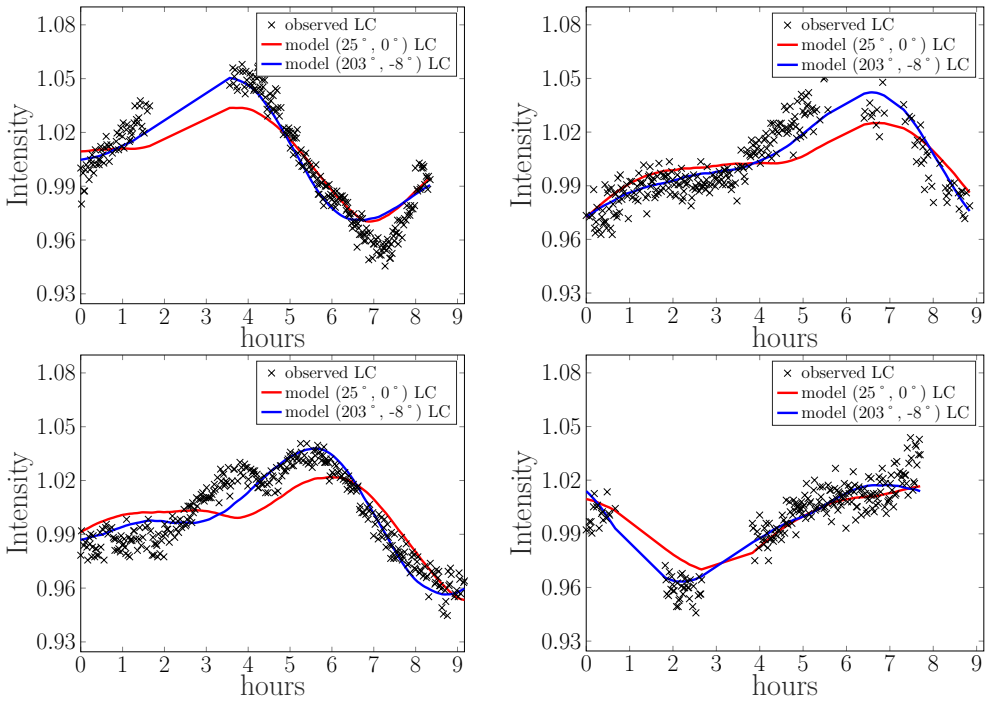

Figure 4.11: Four exemplar light curves of asteroid (81) Terpsichore with two models' fit. The model $(203°, -8°)$ fits the data better.

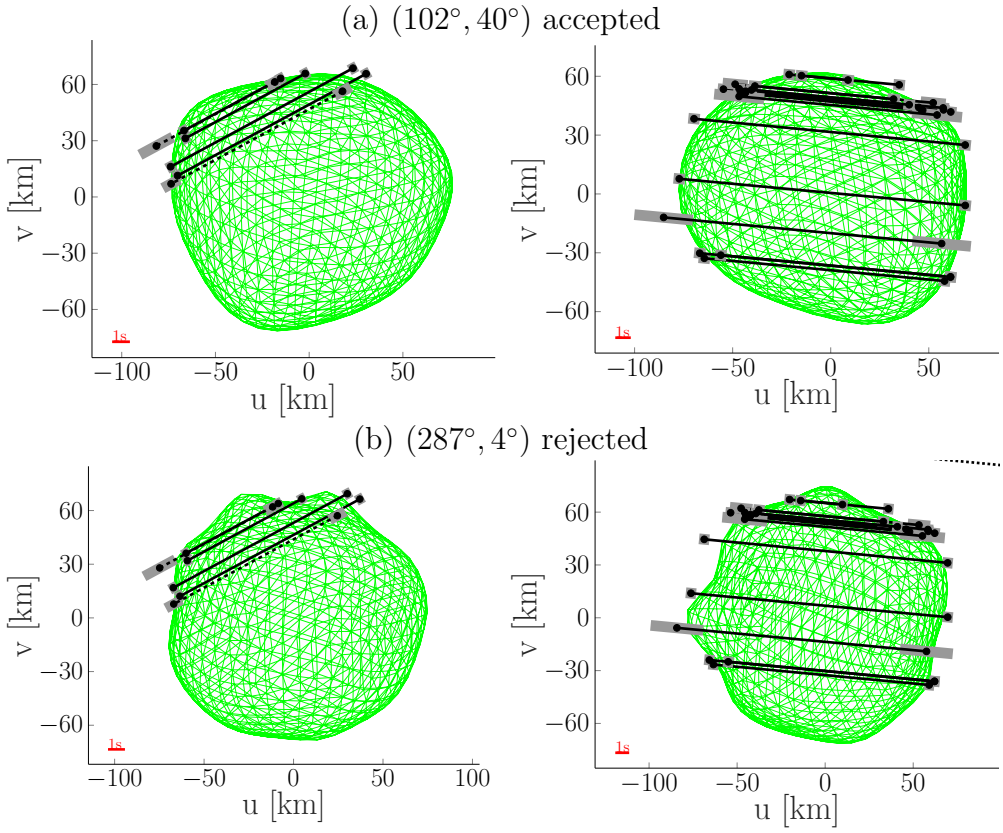

Figure 4.12: Two models of asteroid (145) Adeona from ADAM with projections to two occultations.

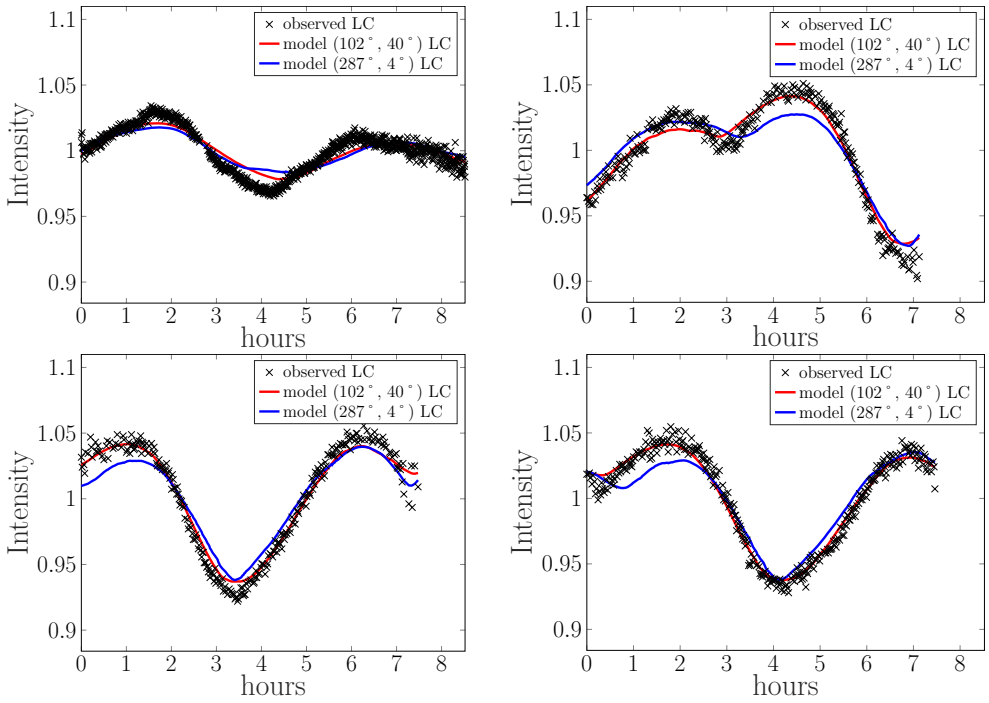

Figure 4.13: Four exemplar light curves of asteroid (145) Adeona with two models' fit. The model $(102°, 40°)$ fits the data better.

position is $(294°, 30°)$.

4.2.4 (420) Bertholda

Asteroid (420) Bertholda has only 3 dense lc, but six observed occultations. The derived period is 10.99 h and has two possible poles from light curves. These are $(262°, 80°)$ and $(98°, 67°)$. From these two models $(262°, 80°)$ better fit both light curves and occultations after shape creation. Fit to occultation differs visually, as can be seen in Fig. 4.16. On the other hand the fit on dense light curves, shown in Fig. 4.17, is visually similar for both models, but the RMS values (0.038 vs 0.040) suggest also the model with pole $(262°, 80°)$. For this model, the final pole position from ADAM is $(264°, 81°)$.

4.2.5 (451) Patientia

Even though asteroid (451) Patientia has 125 dense light curves, we still get eight possible pole positions. And even though we have eight occultations, two of which are dense and cover the whole shape, I was not able to identify uniquely the pole position after shape model creation. The two best pole positions are $(353°, 5°)$ and $(175°, 45°)$. These two models have almost the same fit on both occultations, shown in Fig. 4.18, and light curves, visualized in Fig. 4.19, with the same RMS values. So until new data becomes available, I am not able to determine the correct model and still have the pole ambiguity.

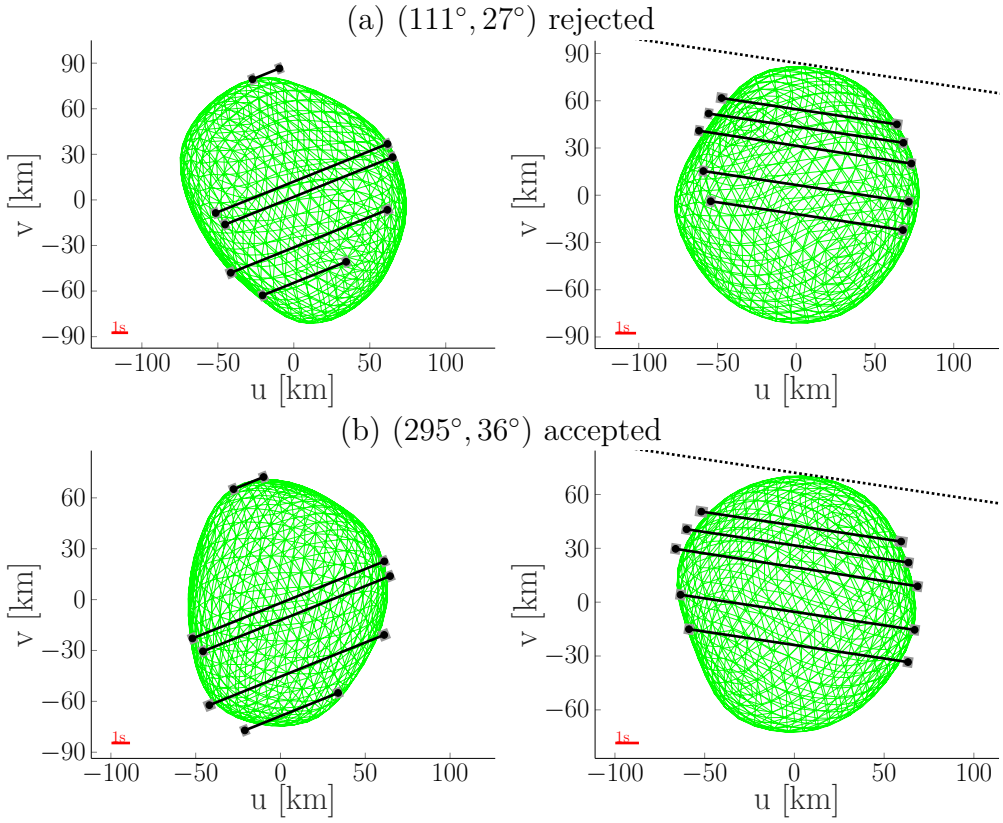

Figure 4.14: Two models of asteroid (308) Polyxo from ADAM with projections to two occultations. The model (295°, 36°) fits the data better.

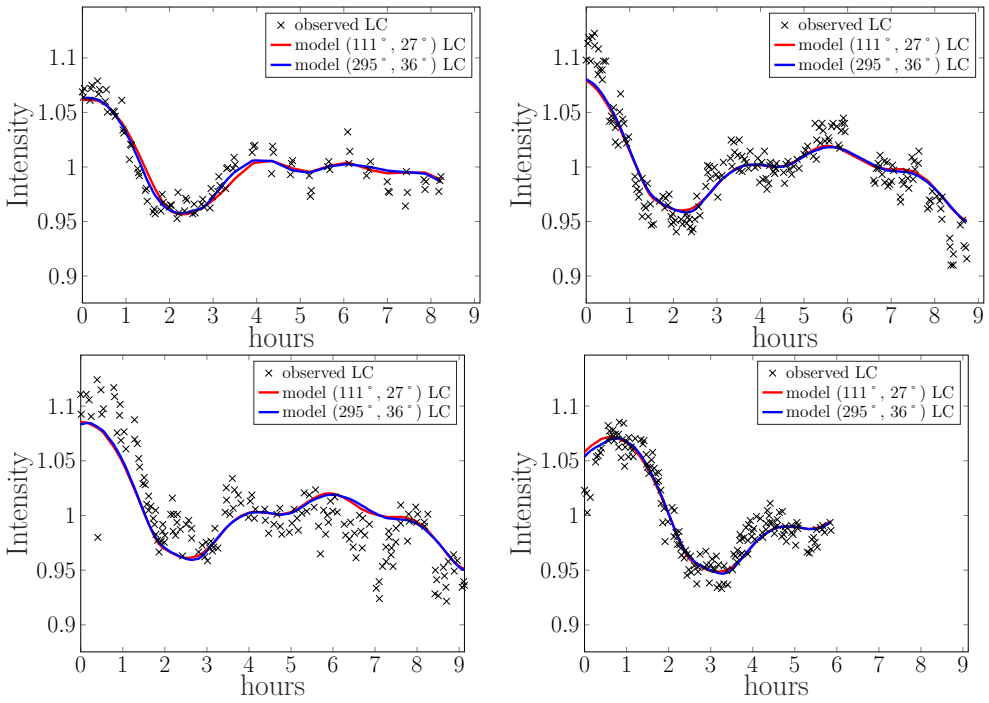

Figure 4.15: Four exemplar light curves of asteroid (308) Polyxo with two models' fit.

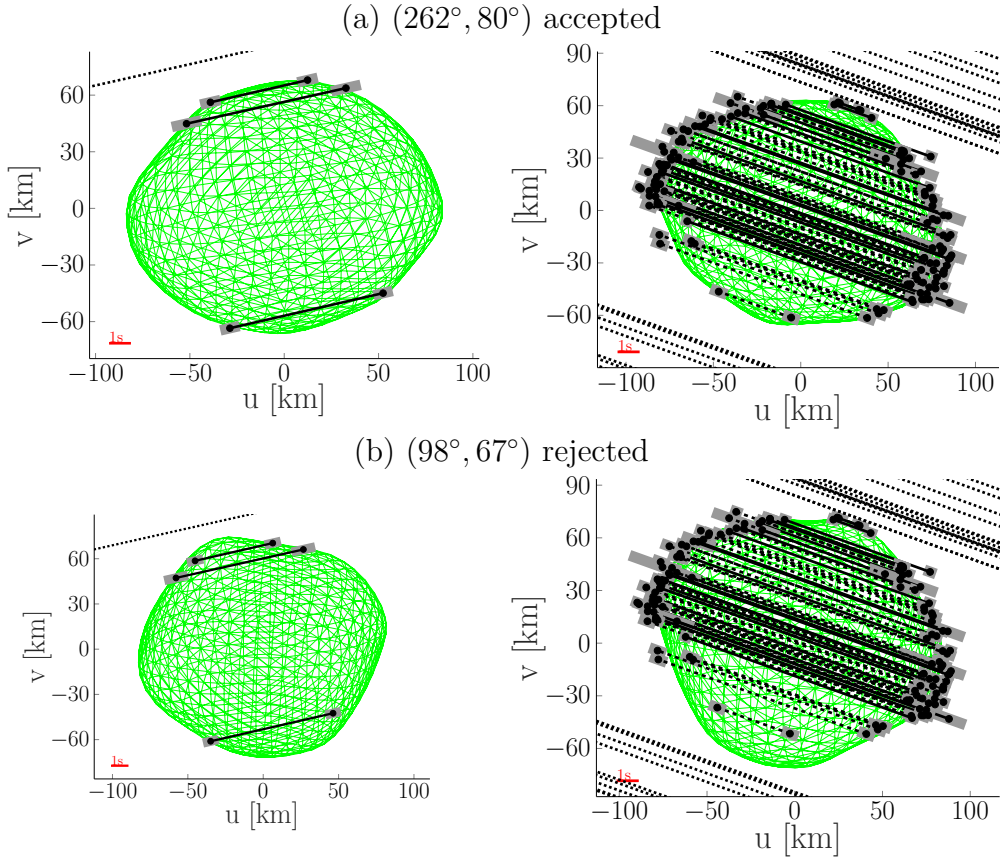

Figure 4.16: Two models of asteroid (420) Bertholda from ADAM with projections to two occultations.

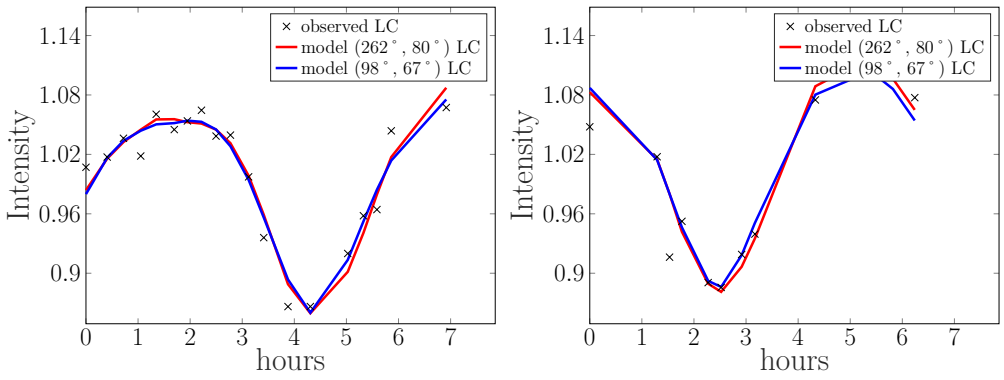

Figure 4.17: Two exemplar light curves of asteroid (420) Bertholda with two models' fit. The model (262°, 80°) fits the data better.

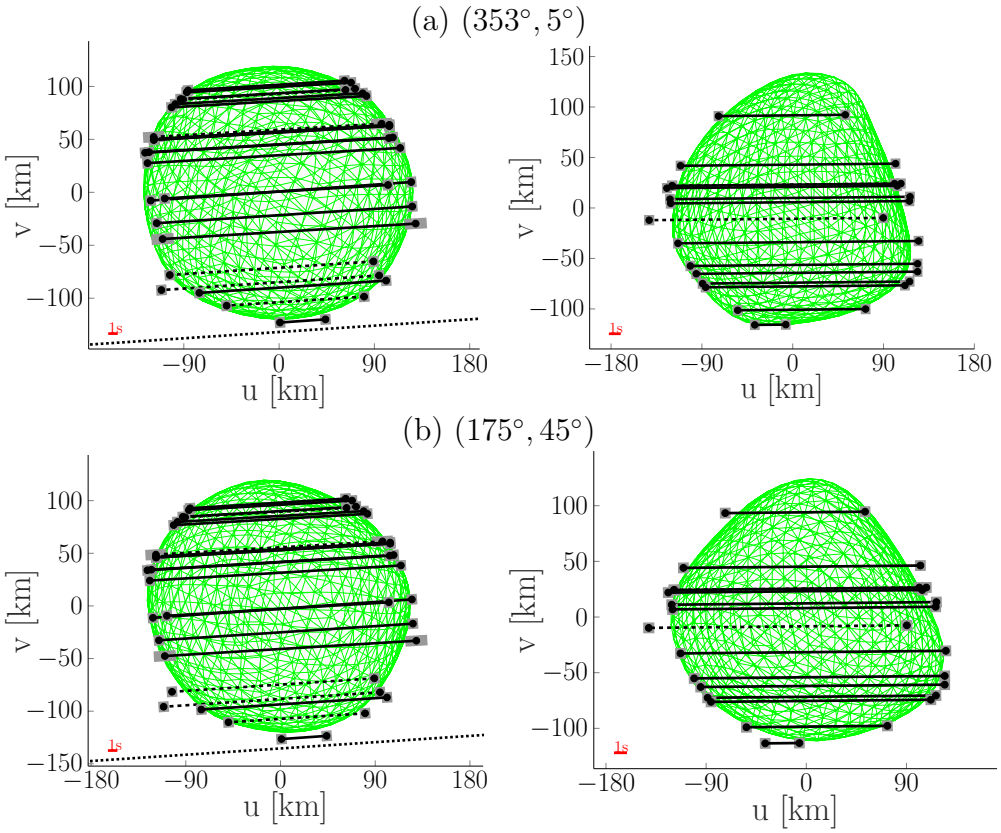

Figure 4.18: Two models of asteroid (451) Patientia from ADAM with projections to two occultations. Both models fit the data similarly.

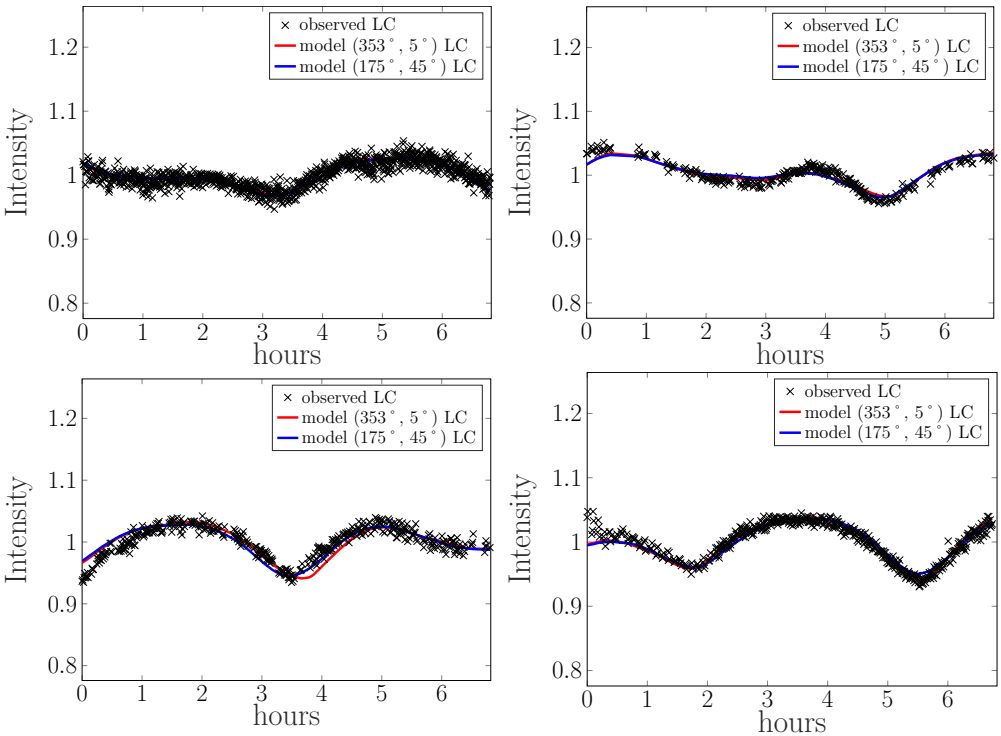

Figure 4.19: Four exemplar light curves of asteroid (451) Patientia with two models' fit. Both models fit the data similarly.

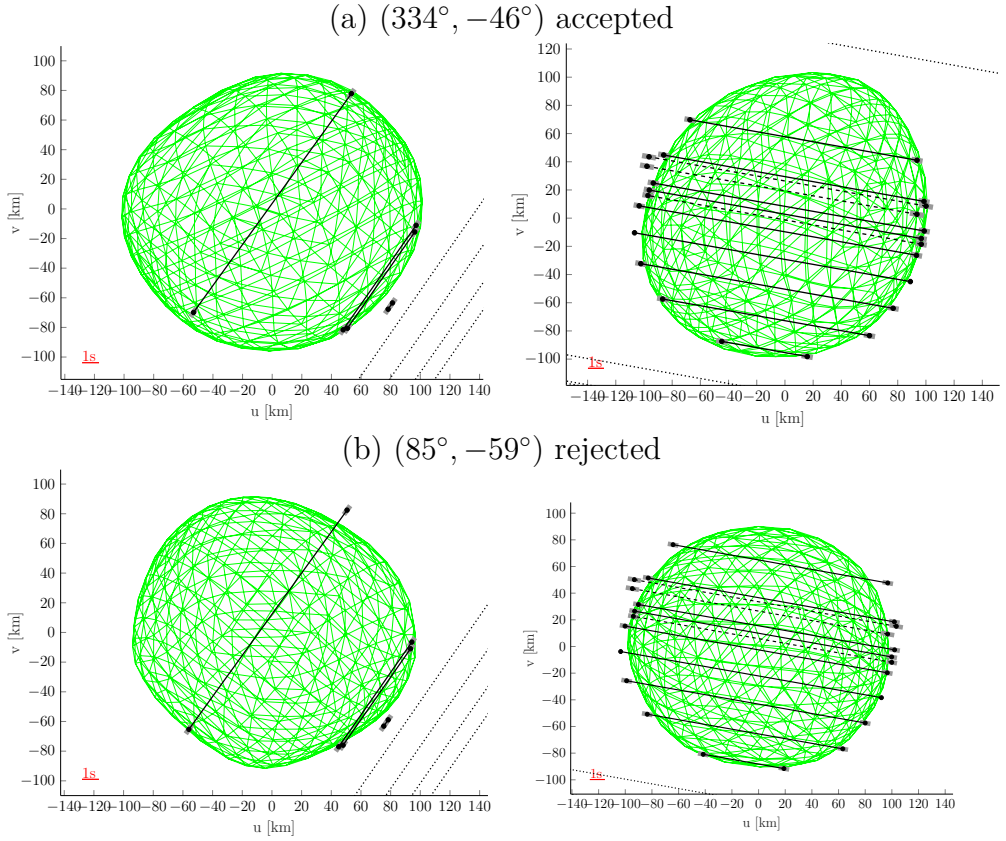

Figure 4.20: Two models of asteroid (702) Alauda from ADAM with projections to two occultations.

4.2.6 (702) Alauda

Asteroid (702) Alauda has 102 light curves and seven occultations. That makes it an asteroid with one of the largest data sets. However, I was still unable to solve the pole ambiguity. From light curves alone I got period 16.70 h and two pole positions (334°, −46°) and (85°, −59°). From these two models, the first fits slightly better on light curves, as can be seen in Fig. 4.21, whereas the other on occultations, shown in Fig. 4.20.

4.2.7 (914) Palisana

This asteroid has a smaller data set with only 13 dense light curves, but it has three occultations with more than two observers. Using light curves to determine the initial parameters I got its period 8.68 h and two pole positions. From those two pole solutions, I have created two models, with one clearly better. The model with pole position (209°, −20°) has an RMS value of 0.030, while the model for pole (29°, −22°) has 0.045. The fitting on two light curves can be seen in Fig. 4.23. Also, the projections on occultations show that the initial pole position (209°, −20°) is the correct one. This can be seen in Fig. 4.22. The final pole position of ADAM convergence is (210°, −24°).

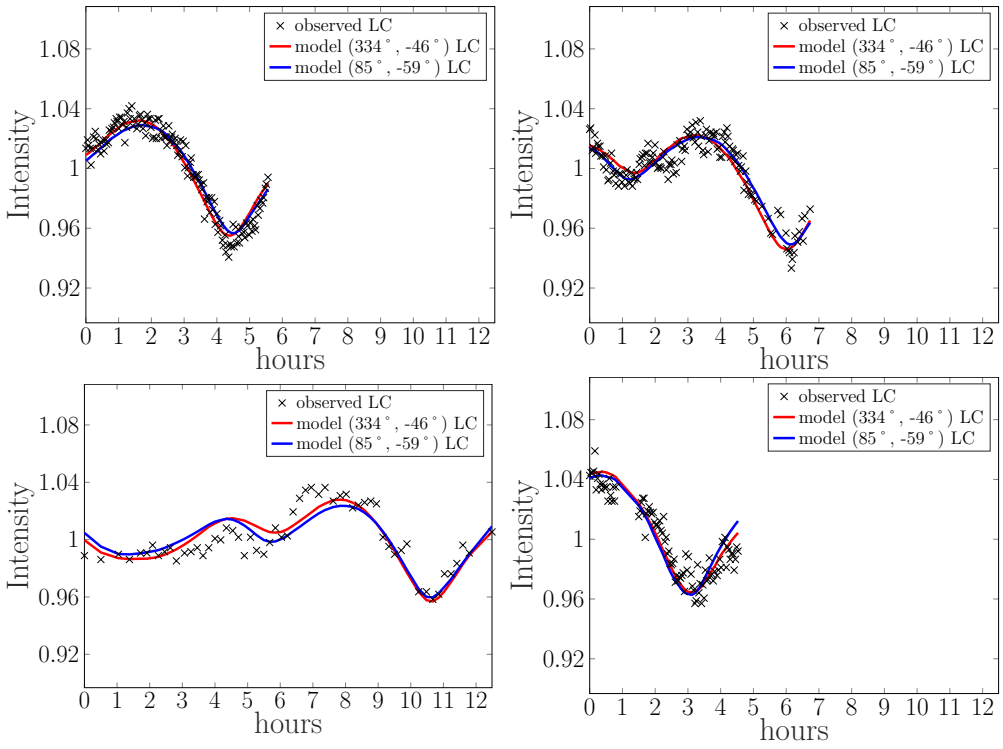

Figure 4.21: Four exemplar light curves of asteroid (702) Alauda with two models' fit. The model $(334°, -46°)$ fits the data better.

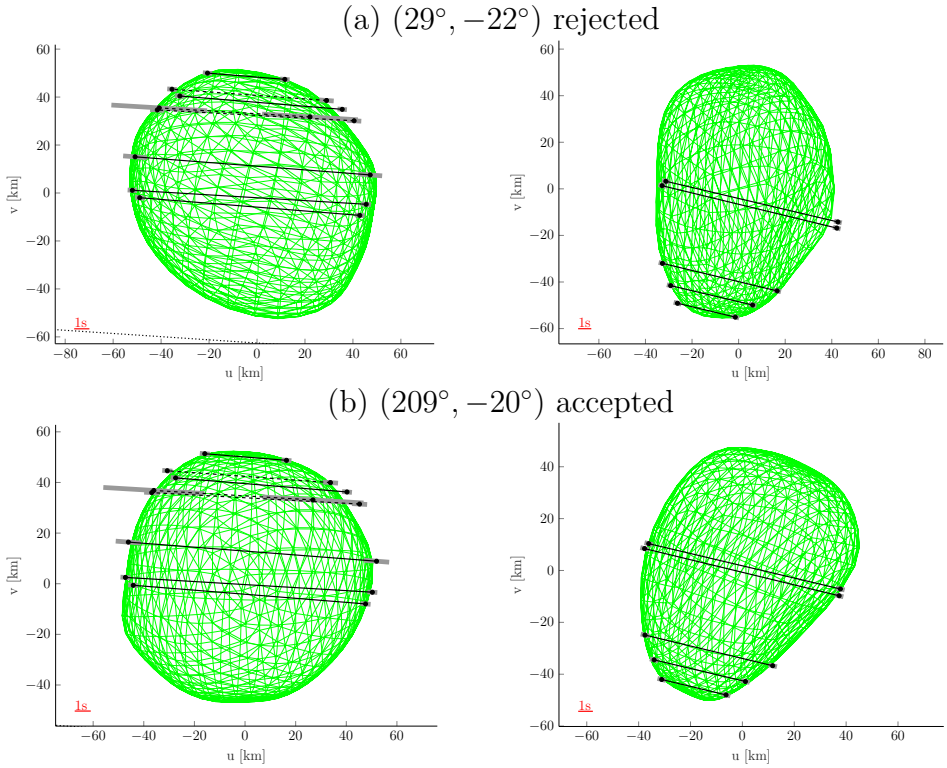

Figure 4.22: Two models of asteroid (914) Palisana created from ADAM, which are identified by their pole position, fitted to two occultations from 12 September 2004 and 3 March 2022.

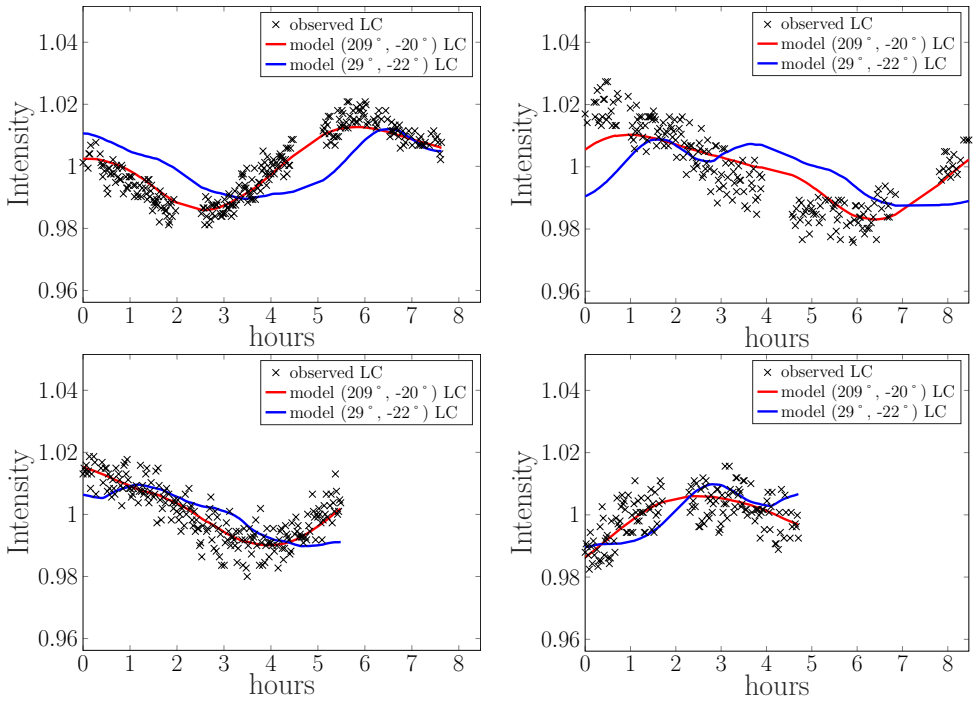

Figure 4.23: Four exemplar light curves of asteroid (914) Palisana with two models' fits. Model $(209°, -20°)$ fits much better than model $(29°, -22°)$.

4.3 Asteroids with non-convex models

The third group contains asteroids with new non-convex models, both with and without a previous model in DAMIT. Their non-convex features are introduced thanks to occultations. Sometimes the non-convex shape is clearly visible from the occultation, as can be seen in Fig. 3.5. But other times the occultations can appear convex and the created model is non-convex. This group contains 22 asteroids, listed in Table 4.4. Some of these asteroids have more possible pole solutions, even after occultation fitting. This ambiguity could be resolved if more observations of occultations are available in the future. As was mentioned before, the light curve fit is very similar for convex and non-convex models, so observations of light curves cannot distinguish between convex and non-convex shapes. Two asteroids in this group already have their model created with occultation in paper Marciniak et al. (2023). These two asteroids are (70) Panopaea and (275) Sapientia. The diameter of these asteroids determined in the paper and by me are in agreement. My derived diameter for asteroid (70) Panopaea is 125.5 ± 1.0 and in the paper, the value is 128 ± 7. For asteroid (275) Sapientia is my diameter 104.8 ± 0.9 and their diameter 103 ± 7. But even though our derived diameters are in agreement, the models are not, because our derived pole positions differ. I will now present all asteroids that had no previous model in DAMIT and one with it.

Table 4.4: List of asteroids with non-convex models with their pole position, equivalent diameter from occultations and from IR and whether they had a previous convex model in DAMIT. There are two types of uncertainty for equivalent diameter one is extremal interval based on possible biggest and smallest model and σ is stndard deviation based on 50 created models.

	Asteroid	pole position	DAMIT	D [km]	σ [km]	D_{IR} [km]	$\sigma_{D_{IR}}$ [km]
(55)	Pandora	(231°, 20°)	YES	$80.7^{+3.1}_{-0.4}$	1.3	84.8	2.5
(70)	Panopaea	(66°, 16°)	YES	$125.5^{+2.2}_{-1.9}$	1.0	127.9	0.7
(78)	Diana	(32°, 8°)	NO	$111.8^{+4.3}_{-4.2}$	12.0	160.1	45.7
(105)	Artemis	(44°, 15°)	YES	$106.5^{+6.1}_{-4.3}$	1.2	119.0	17.0
(115)	Thyra	(196°, 83°)	YES	$82.5^{+3.0}_{-0.0}$	4.2	55.1	11.2
(135)	Hertha	(270°, 48°)	NO	$81.8^{+3.9}_{-2.1}$	2.0	71.0	2.7
(138)	Tolosa	(199°, − 2°)	YES	$52.3^{+1.6}_{-1.2}$	0.6	52.9	1.0
(153)	Hilda	(339°, − 11°)	NO	$177.3^{+8.7}_{-1.9}$	5.4	218.8	7.0
(200)	Dynamene	(328°, 45°), (162°, 47°)	NO	$125.1^{+1.7}_{-2.3}$	0.8	128.3	1.9
(205)	Martha	(30°, 22°)	NO	$64.1^{+2.1}_{-3.8}$	2.1	77.0	0.6
(258)	Tyche	(52°, 11°)	YES	$56.0^{+0.6}_{-2.9}$	0.5	65.8	2.1
(275)	Sapientia	(86°, 65°)	YES	$104.8^{+2.3}_{-3.0}$	0.9	95.5	1.1
(363)	Padua	(183°, 41°)	NO	$86.3^{+0.7}_{-0.6}$	0.5	86.0	0.7
(375)	Ursula	(325°, − 42°), (123°, − 17°)	NO	$195.9^{+6.4}_{-5.9}$	1.2	189.4	54.8
(411)	Xanthe	(84°, 1°)	NO	$78.1^{+10.6}_{-2.5}$	4.8	76.3	3.2
(423)	Diotima	(348°, 0°)	NO	$186.1^{+9.8}_{-12.7}$	3.7	175.9	3.9
(506)	Marion	(259°, − 44°)	NO	$104.1^{+3.7}_{-0.3}$	2.0	111.3	3.1
(521)	Brixia	(307°, 22°)	YES	$115.5^{+6.6}_{-3.8}$	1.2	107.2	0.5
(554)	Peraga	(269°, − 66°), (70°, − 70°)	YES	$102.2^{+3.6}_{-3.1}$	3.5	94.9	23.2
(788)	Hohensteina	(259°, 26°)	NO	$99.0^{+0.0}_{-0.0}$	2.1	111.3	0.8

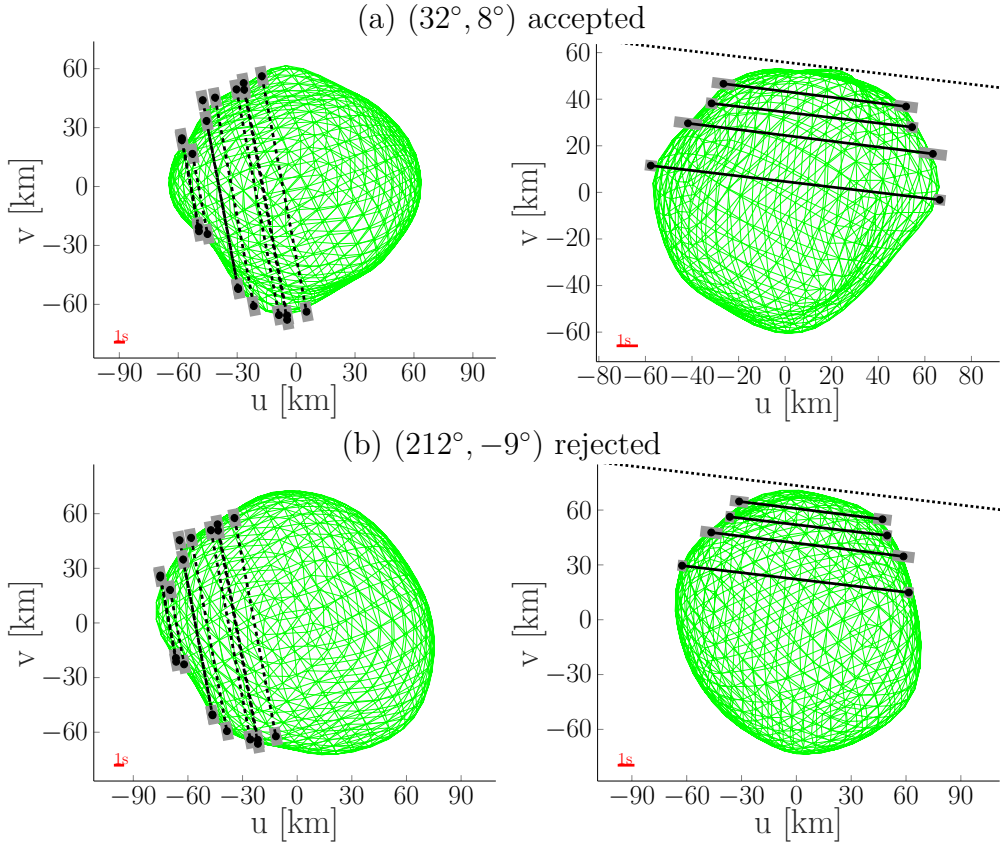

Figure 4.24: Two models of asteroid (78) Diana from ADAM with projections to two occultations.

4.3.1 (78) Diana

The data set of Asteroid (78) Diana belongs between smaller ones. It has only 13 dense light curves and three occultations, two of which have four observers. However I was still able to create a new model that fits the data and determine uniquely its period and pole position. From light curves is its period 7.29 h and has two pole positions: $(32°, 8°)$ and $(212°, -9°)$. After model creation, I was able to determine that the initial pole position $(32°, 8°)$ is better and its final value is $(29°, 4°)$. This cannot be seen from occultation fitting in Fig. 4.24, only the light curve fit shows, even with a close RMS value of 0.036 for the first pole and 0.038 for the second, that the first pole is indeed the correct one. The light curve fit is visualized in Fig. 4.25.

4.3.2 (135) Hertha

Hertha has 42 light curves, but only two occultations and one of them with only three observers. However the other occultations are densely covered in more than half of the model and around one distinct non-convex feature. From its light curves, I determined the period to be 8.40 h and got again ambiguous pole positions. From its two pole positions $(270°, 48°)$ and $(91°, 44°)$, the first one is clearly a better fit to data after model creation. It can be seen especially from occultations in Fig. 4.26. Here model $(270°, 48°)$ has an almost perfect fit to the occultations, the non-convex feature included, whereas with as the other one

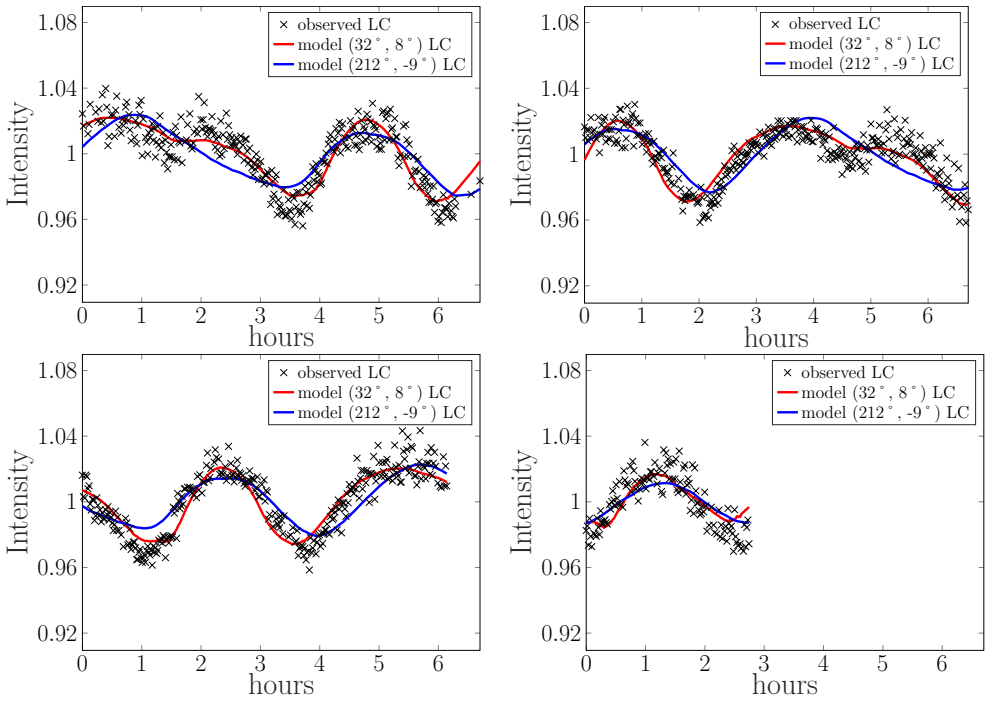

Figure 4.25: Four exemplar light curves of asteroid (78) Diana with two models' fit. The model $(32°, 8°)$ fits the data better.

differs a lot from the first occultation. The light curve fit is visually similar for both models, as is shown in Fig. 4.27, but the RMS value is better for the first model with 0.038 over 0.042. The final pole position from ADAM is $(273°, 60°)$.

4.3.3 (153) Hilda

For asteroid (135) Hilda I have available large data set. With 35 dense light curves, it would be ordinary, but with 6 usable occultations, it is above average. By starting with light curves alone I got its period as 5.96 h and two possible pole positions $(339°, -11°)$ and $(160°, -25°)$. Modelling with occultation give slightly non-convex shapes with one almost perfect fit to the occultations, whereas the other one has some discrepancies, as can be seen in Fig. 4.28. The same goes with the light curves fit visualized in Fig. 4.29, along with its RMS value 0.039 vs 0.042. With this I can conclude that the pole position $(339°, -11°)$ is the correct. The final pole position from ADAM is $(340°, -11°)$.

4.3.4 (200) Dynamene

Asteroid (200) Dynamene has 19 dense light curves and only one occultation. This puts Dynamene between asteroids with smaller data set. Probably for this reason, I got five possible pole positions and even after modelling wasn't able to identify the correct one between the two best. So for this asteroid I have two possible model with period 37.40 h and pole positions $(162°, 47°)$ and $(328°, 45°)$. Fitting to the one occultation is shown in Fig. 4.30, where we can see, that both models corresponds to observation. Fitting of light curves is plotted in Fig. 4.31 and it also shows similar fit for both models. So I am not able to choose the

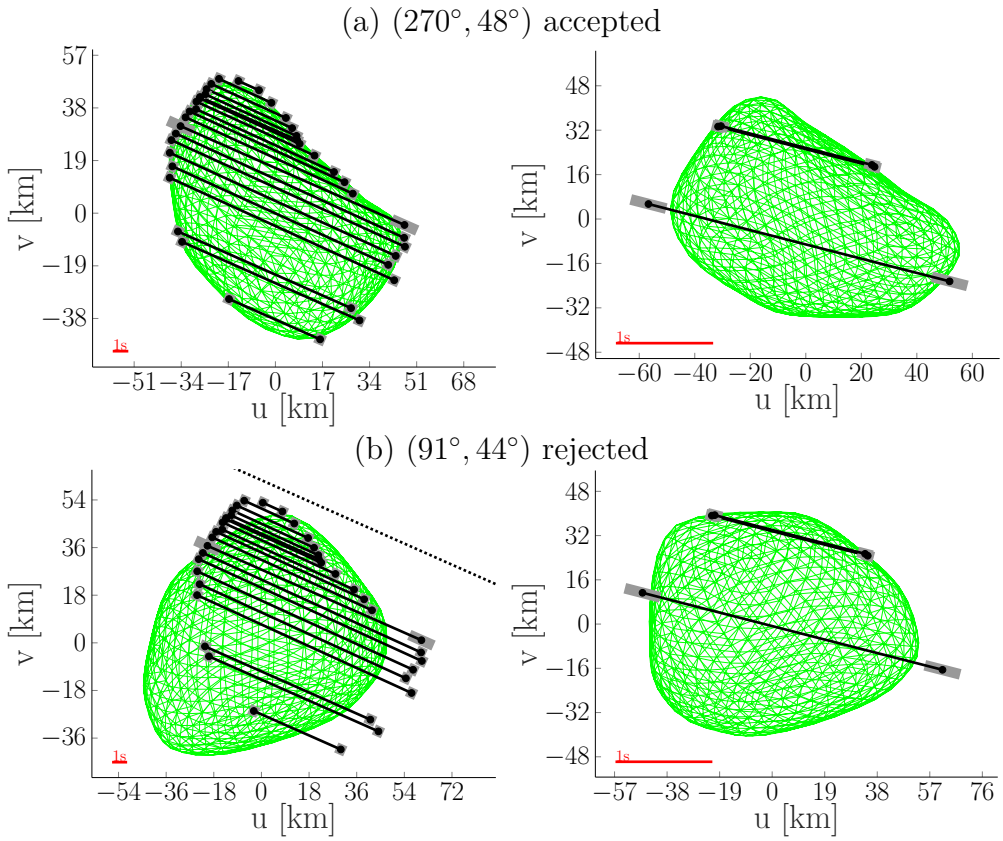

Figure 4.26: Two models of asteroid (135) Hertha from ADAM with projections to two occultations.

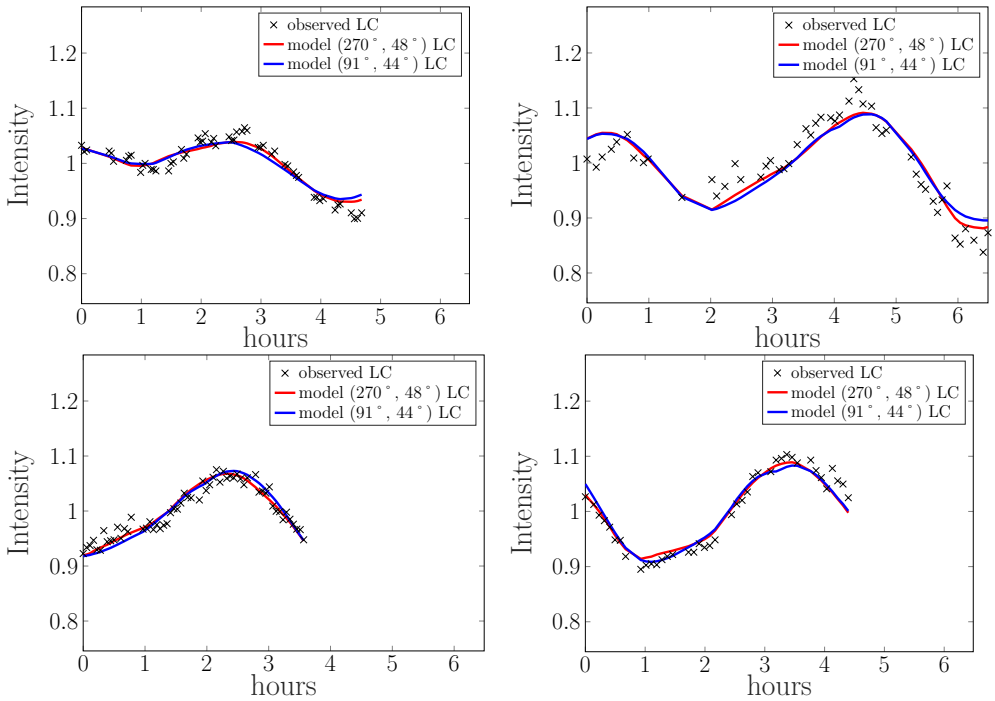

Figure 4.27: Four exemplar light curves of asteroid (135) Hertha with two models' fit. The model (270°, 48°) fits the data better.

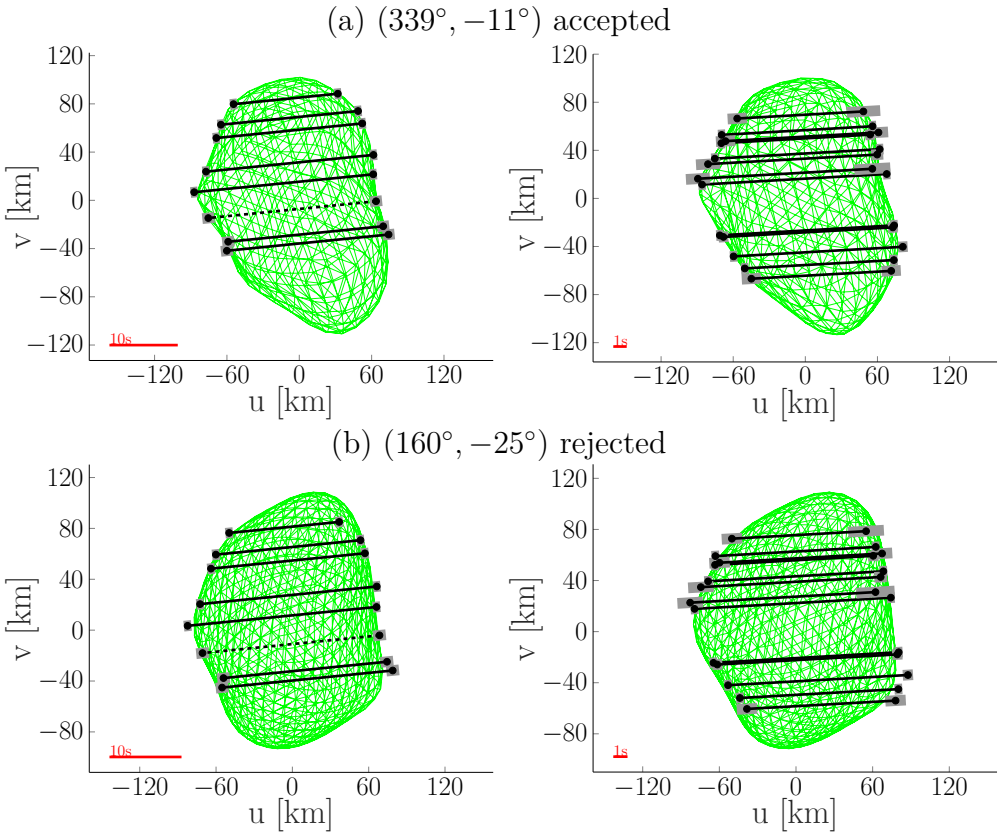

Figure 4.28: Two models of asteroid (153) Hilda from ADAM with projections to two occultations.

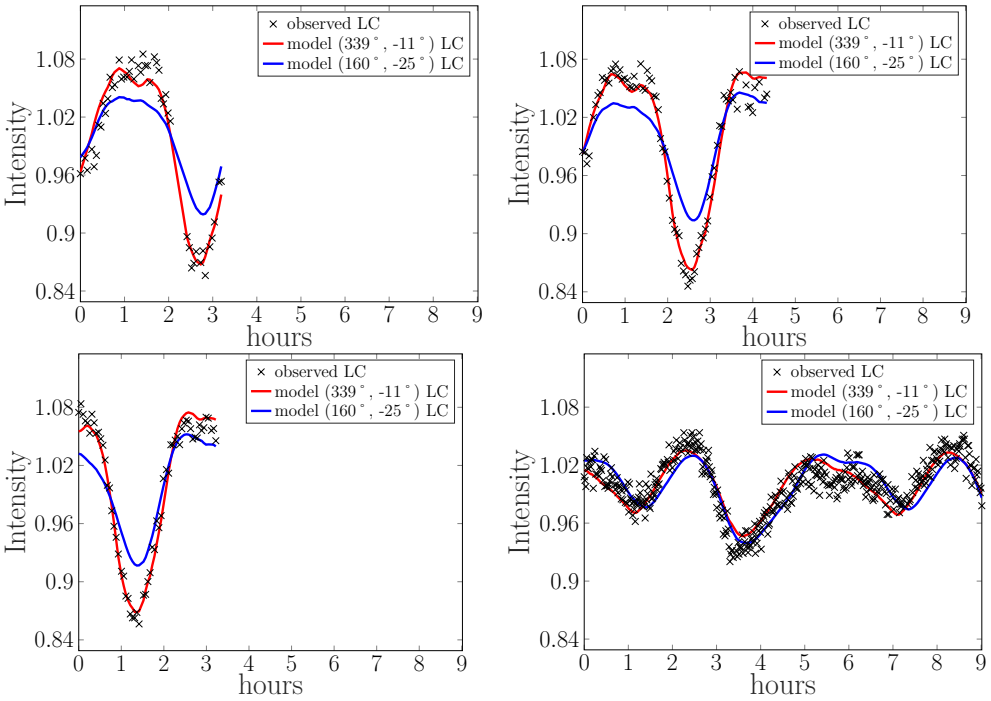

Figure 4.29: Four exemplar light curves of asteroid (153) Hilda with two models' fit. The model (339°, −11°) fits the data better.

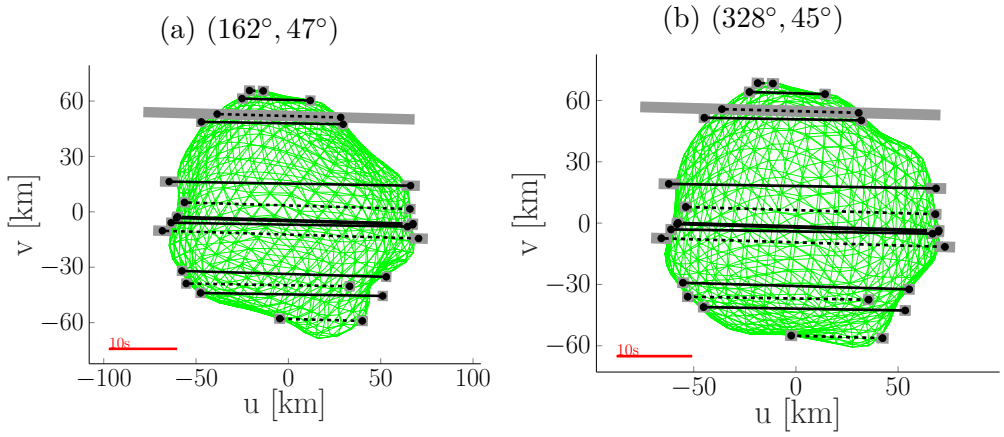

Figure 4.30: Two models of asteroid (200) Dynamene from ADAM with projections to occultation. Both models fit the data similarly.

correct pole position until new data are available.

4.3.5 (205) Martha

Data set for asteroid (205) Martha includes 28 dense light curves but only one occultations. In addition this occultation has half the observers close to one another around the top of model projection and the others are visual shifted to each other. So model created using this occultation is not the most precise one, but still improvement over convex model from light curves and good starting point for future modelling with more occultations. From light curves I got period of 14.90 h and two pole positions $(201°, 18°)$ and $(30°, 22°)$. After creating their model, both have similar fit to occultation as can be seen in Fig. 4.32, but the second pole has better fit to light curves as can be seen in Fig. 4.33. Therefore I will consider the pole position $(30°, 22°)$ to be the correct one until new observation will be available.

4.3.6 (258) Tyche

Now the asteroid (258) Tyche, which has a small data set. Only 14 observed light curves and one occultation, which is shown in Fig. 3.5 and has a distinct non-convex feature. It had two previous models in DAMIT, both of them convex, which suggests that they cannot fit to the occultation. And we can see this in fact in Fig. 4.34. The determined period is 10 h and only one pole position was found. The model for the initial pole $(52°, 11°)$ fits both observed light curves and occultation. This can be seen in Fig. 4.35 for light curves and Fig. 4.36 for occultation. Final pole position from ADAM is $(51°, 8°)$.

4.3.7 (363) Padua

This asteroids also has a small data set. It contains only six dense light curves and one occultation, which does not cover the whole shape, but is densely observed. So I again got two different pole position from light curve: $(183°, 41°)$ and $(360°, 25°)$

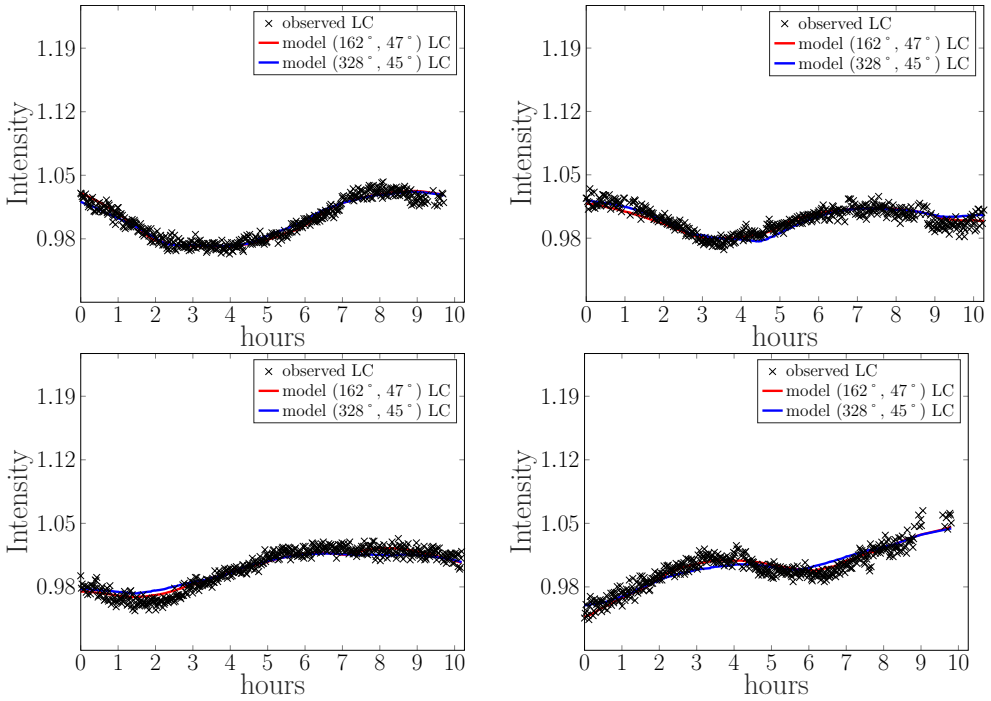

Figure 4.31: Four exemplar light curves of asteroid (200) Dynamene with two models' fit. Both models fit the data similarly.

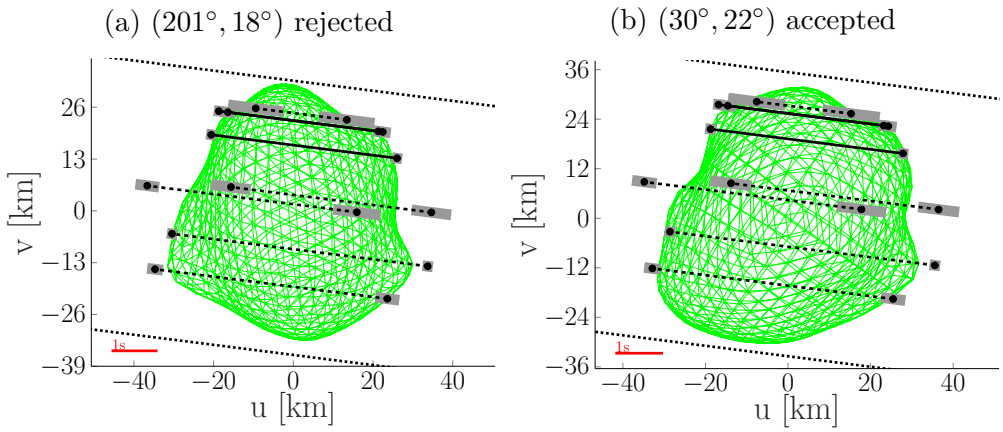

Figure 4.32: Two models of asteroid (205) Martha from ADAM with projections to occultation.

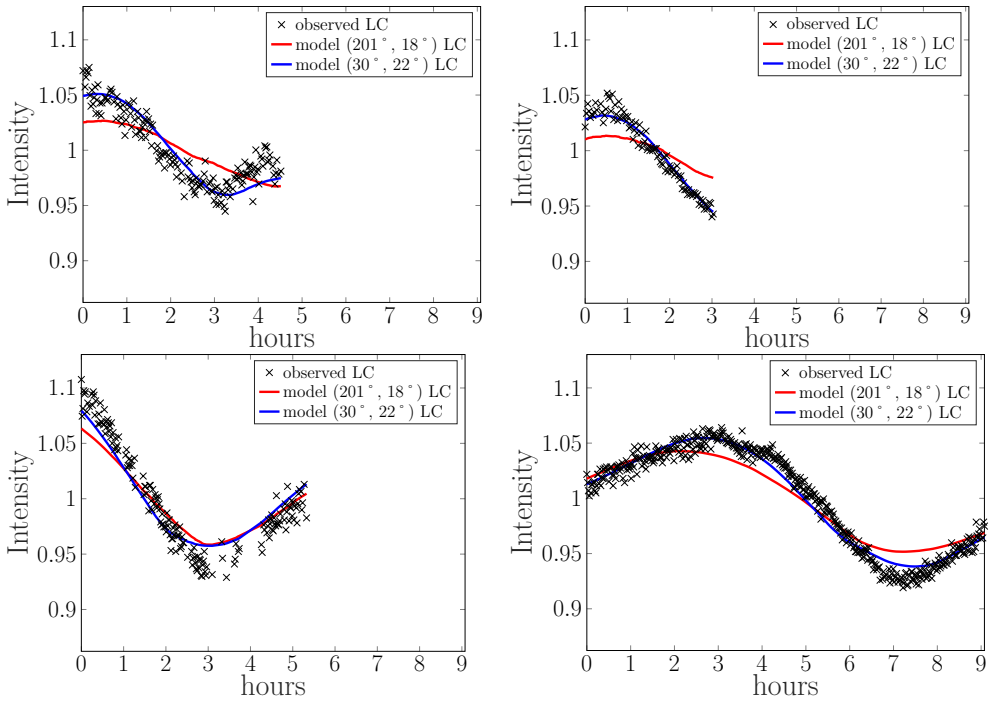

Figure 4.33: Four exemplar light curves of asteroid (205) Martha with two models' fit. The model $(30°, 22°)$ fits the data better.

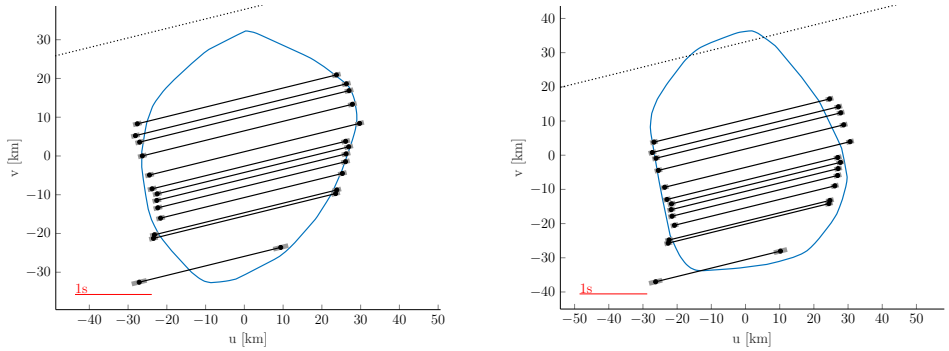

Figure 4.34: Two models of asteroid (258) Tyche from DAMIT with projections to two occultations.

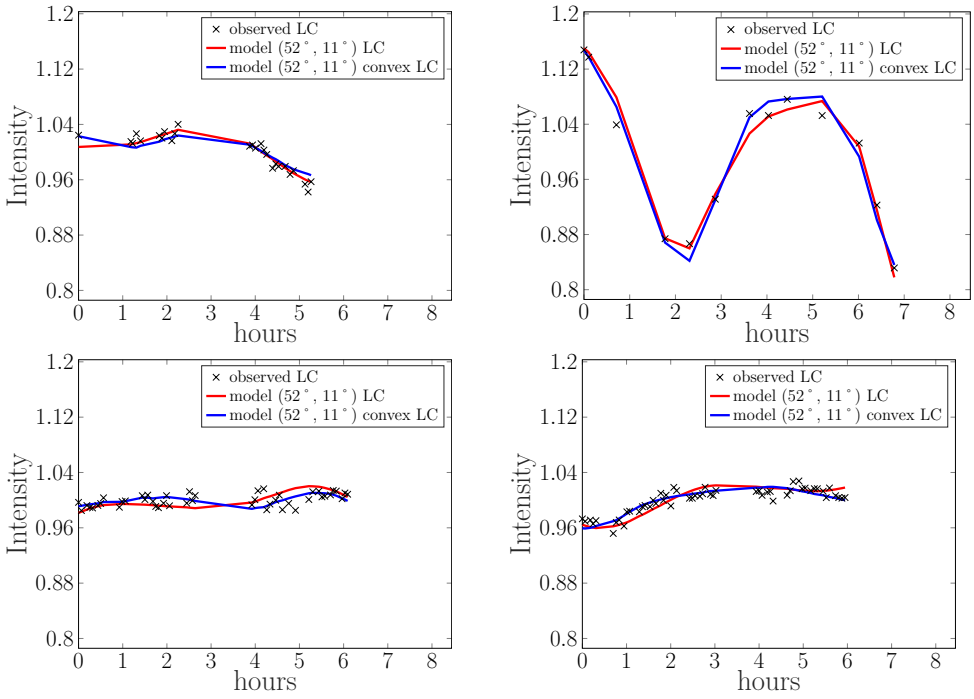

Figure 4.35: Four exemplar light curves of asteroid (258) Tyche with model's fit. One is convex from light curves alone the other non-convex from occultation and light curves. But both model have similar fit.

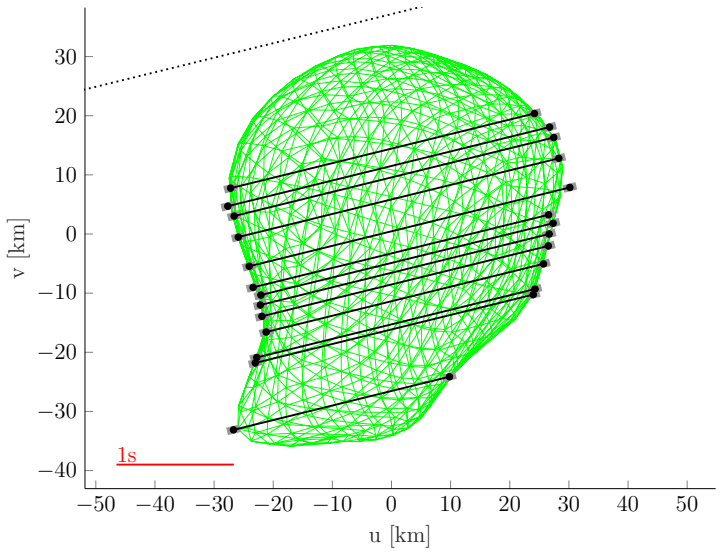

Figure 4.36: Occultation of asteroid (258) Tyche with model from ADAM.

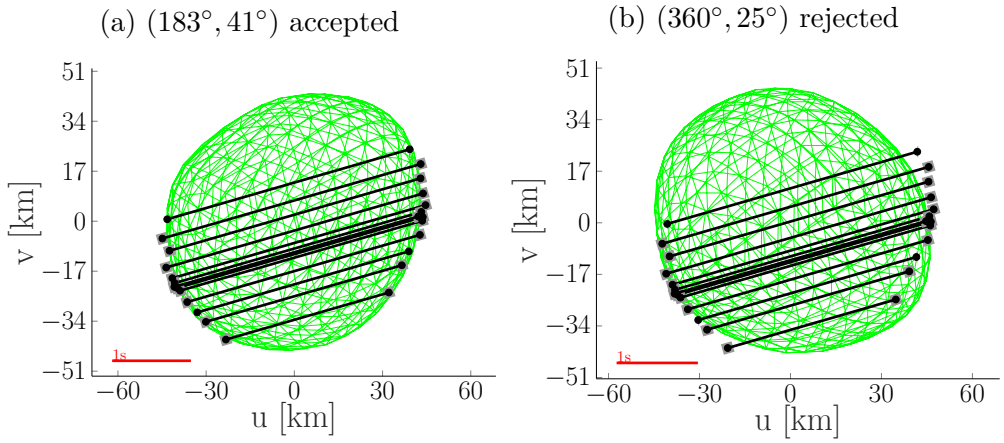

Figure 4.37: Two models of asteroid (363) Padua from ADAM with projections to occultation.

with the period 8.40 h. After modeling the occultation along with the light curves I was able to identify the correct pole position among them. It can be seen from both the occultation fit in Fig. 4.37 and the light curves fit in Fig. 4.38 with the RMS values 0.030 and 0.032. And the final pole position from ADAM is $(180°, 39°)$.

4.3.8 (375) Ursula

For asteroid (375) Ursula there are 26 measured light curves and six observed occultation. This is above average for occultation, but not in light curves. This is probably the reason why I got six possible pole positions with period 16.90 h from light curves. And unfortunately, I was not able to find the one correct pole position with occultation. Here I will present the fit of two best positions. These are $(325°, -42°)$ and $(123°, -17°)$. The both have similar fit to occultations as shown in Fig. 4.39. Also light curves fit is not definite, as can be seen in Fig. 4.40, even the RMS values are almost the same: 0.038 vs 0.039.

Asteroid Ursula is a parent body of the asteroid Ursula family. And we can actually see a crater in model with pole position $(123°, -17°)$, which could be the residue from the collision that created the family. The whole shape model can bee seen in Fig. 4.41.

4.3.9 (411) Xanthe

Asteroid (411) Xanthe has only 11 dense light curves and one occultation. But I was still able to create a correct model, that solves the pole ambiguity from light curves. The period of this asteroid is 7.20 h and its two possible pole positions are $(84°, 1°)$ and $(267°, 10°)$. Neither of the two model has a perfect fit to the light curves as is visualized in Fig. 4.43, but their fit to the occultation in Fig. 4.42 clearly shows that model with pole$(84°, 1°)$ is the correct one. So even when we can say which model is better, it is still not a correct one. Because even though the model fits occultations, fit to light curves is worse than from convex model. So I was not able to find the correct model. This could be for several reasons. Either the data are unreliable, which could possibly be the case with light curves,

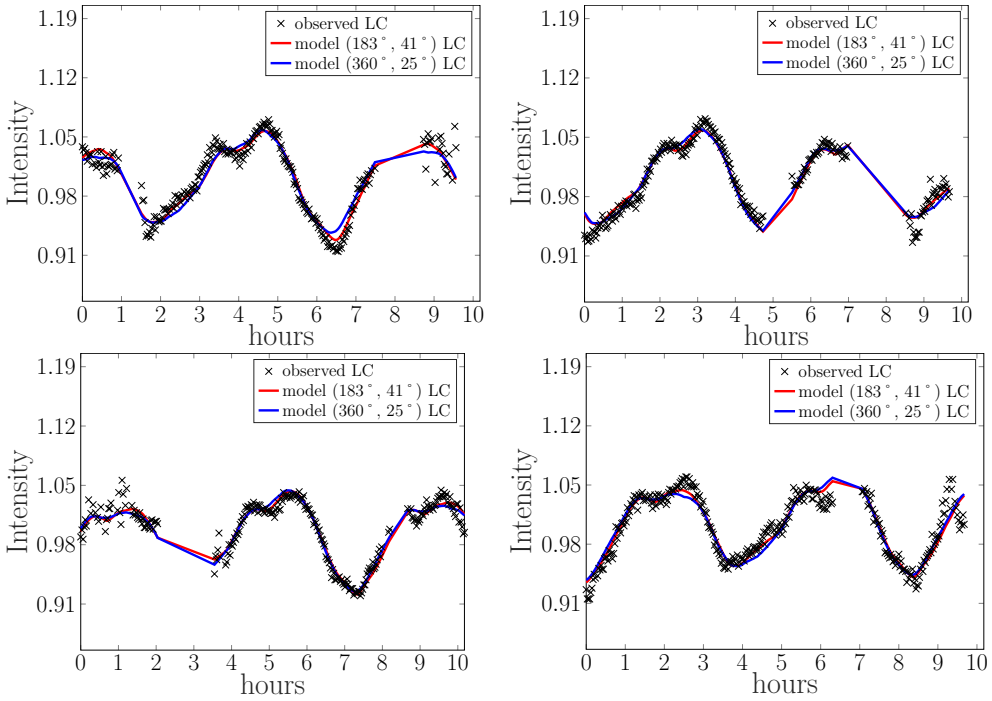

Figure 4.38: Four exemplar light curves of asteroid (363) Padua with two models' fit. The model $(183°, 41°)$ fits the data better.

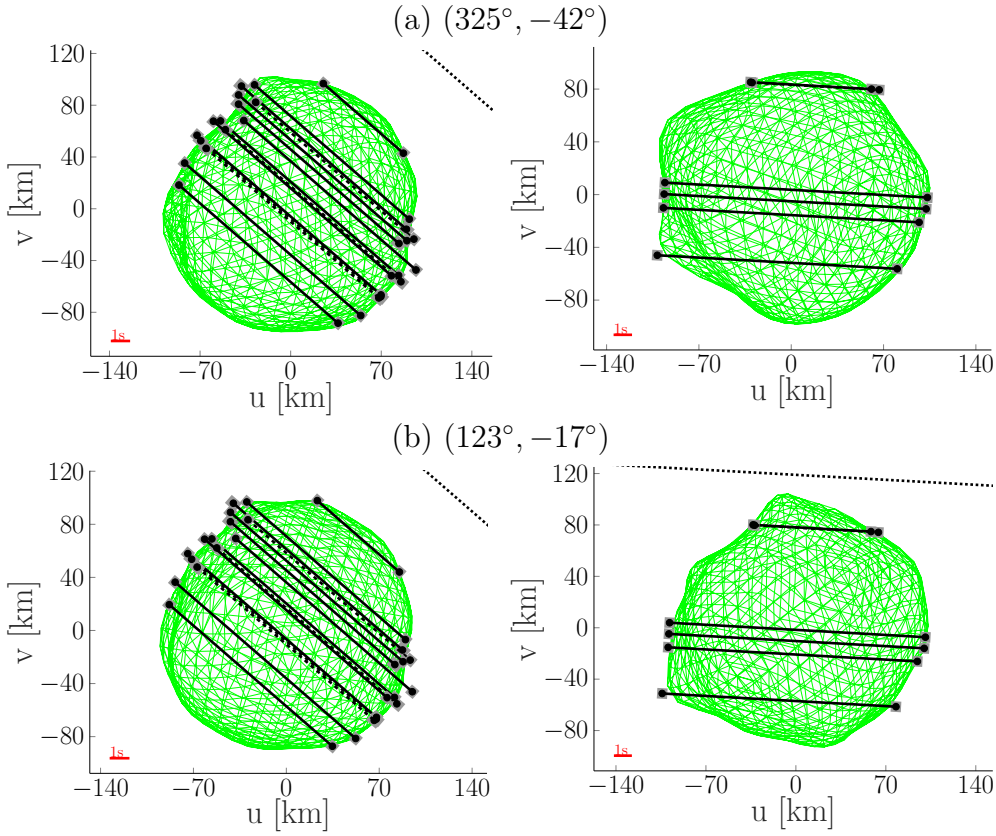

Figure 4.39: Two models of asteroid (375) Ursula from ADAM with projections to two occultations. Both models have similar fit to the data.

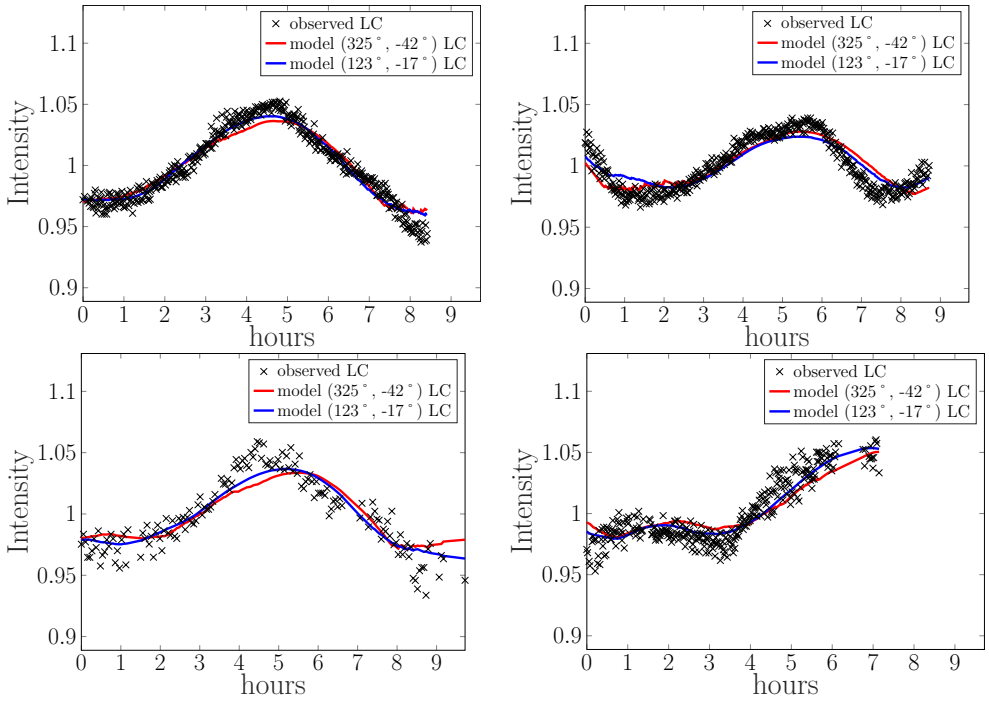

Figure 4.40: Four exemplar light curves of asteroid (375) Ursula with two models' fit. Both models have similar fit to the data.

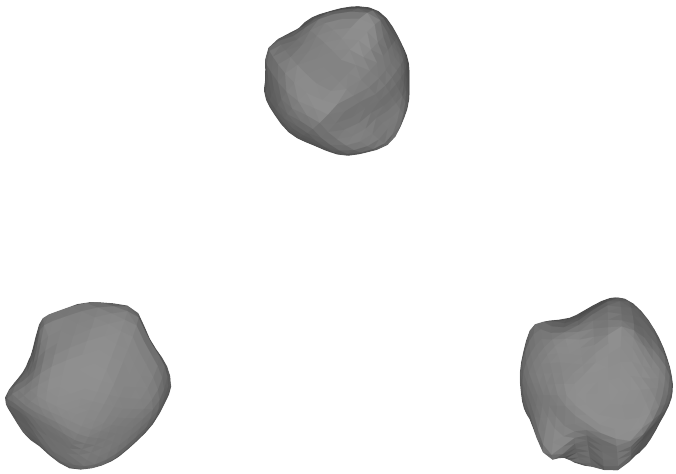

Figure 4.41: Visualization of a model of asteroid (375) Ursula with pole position $(123°, -17°)$ from ADAM. We can see a crater on the surface of the asteroid.

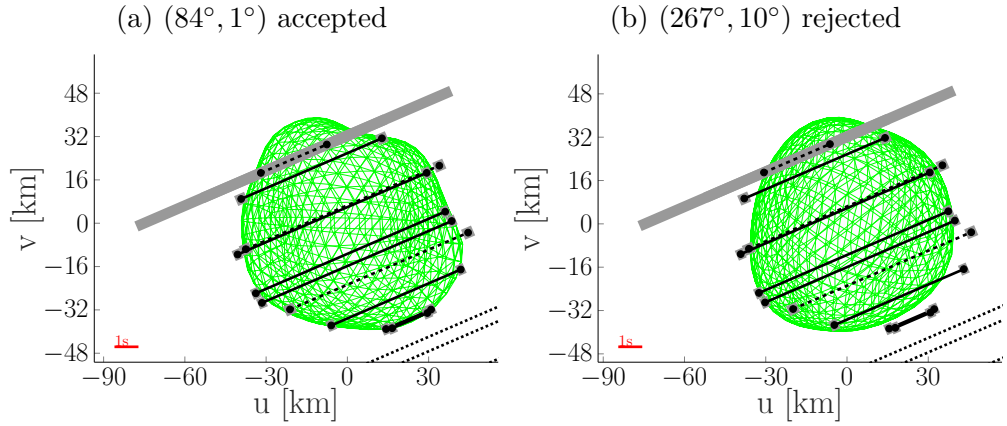

Figure 4.42: Two models of asteroid (411) Xanthe from ADAM with projections to occultation.

because not even the convex model has a got fit. Another reason could be that our modelling is wrong. We assume constant distribution of albedo on asteroid surface. That is almost never true, bu usually the variations are small enough. But if the difference in albedo was large on the asteroid, it could explain the difference between measured and theoretical light curves.

4.3.10 (423) Diotima

Asteroid (423) Diotima has on of the largest data sets. It includes 58 dense light curves and nine occultations. Period determined from light curves is 4.78 h with two pole positions: $(348°, 1°)$ and $(170°, 28°)$. Fortunately, after creating model using occultations for both of them, one model correspond to the occultations much better than the other one, as is shown in Fig. 4.44. Fit to the light curves in Fig. 4.45 is still similar for both of them, but I was able to identify the probably correct pole position as $(348°, 1°)$. Final pole position from ADAM is $(350°, 0°)$

4.3.11 (506) Marion

Data set of (506) Marion is among the smaller one. It contains only 18 dense light curve and one occultation. But the occultation is covered by observations along the whole length. So from the light curves I determined the period to be 13.55 h and with it two possible pole positions $(67°, -14°)$ and $(259°, -44°)$. After model creation the fit to light curves, as is shown in Fig. 4.47, was not good for either of the model and with the same RMS 0.053 for both of them . With the occultation has model $(259°, -44°)$ slightly better fit. But I still cannot say that my model is the correct one, because of the fit to light curves. Unfortunately, I was not able to create a better model. The fit to the occultation is in Fig. 4.46.

4.3.12 (788) Hohensteina

This asteroid has 25 dense light curves and three occultations. It was presented earlier in this chapter as an example of regularization instability. This instability usually suggests that the data is insufficient, or as in this case that improving the

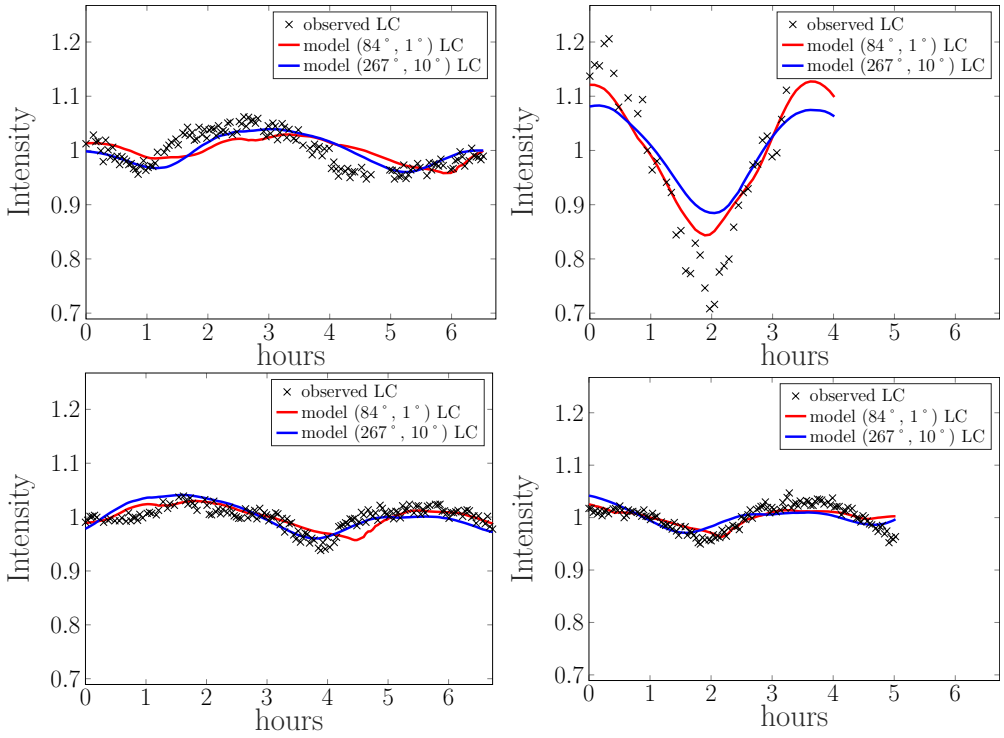

Figure 4.43: Four exemplar light curves of asteroid (411) Xanthe with two models' fit. The model $(84°, 1°)$ fits the data better.

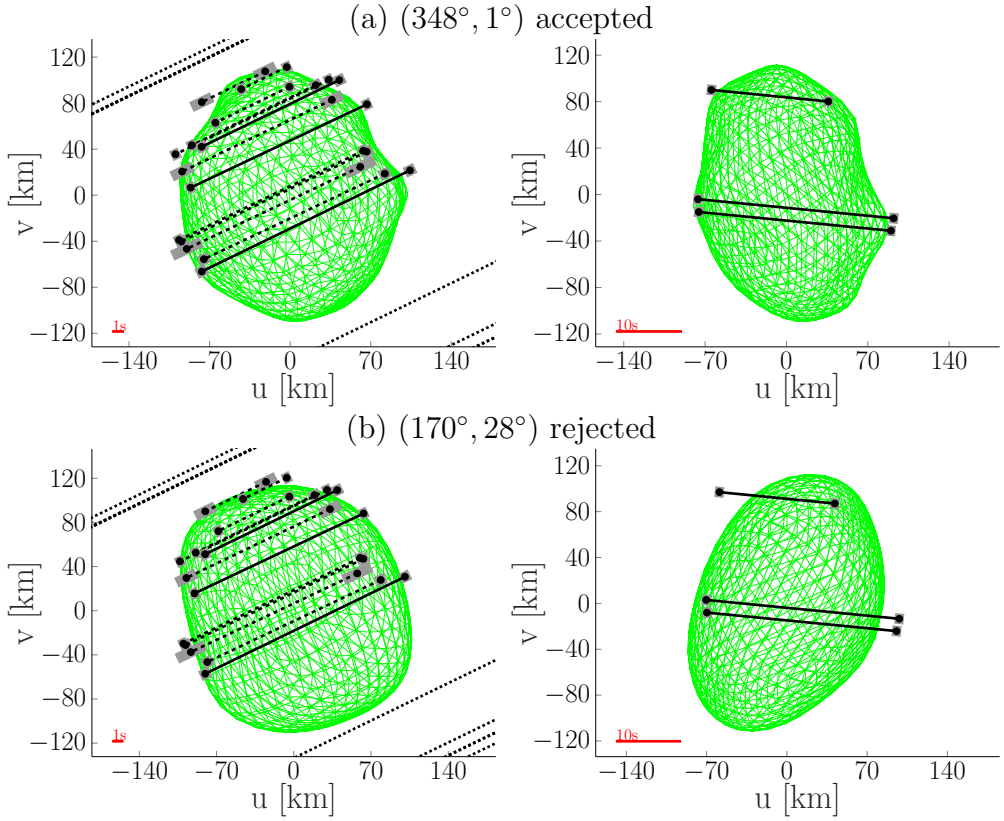

Figure 4.44: Two models of asteroid (423) Diotima from ADAM with projections to two occultations.

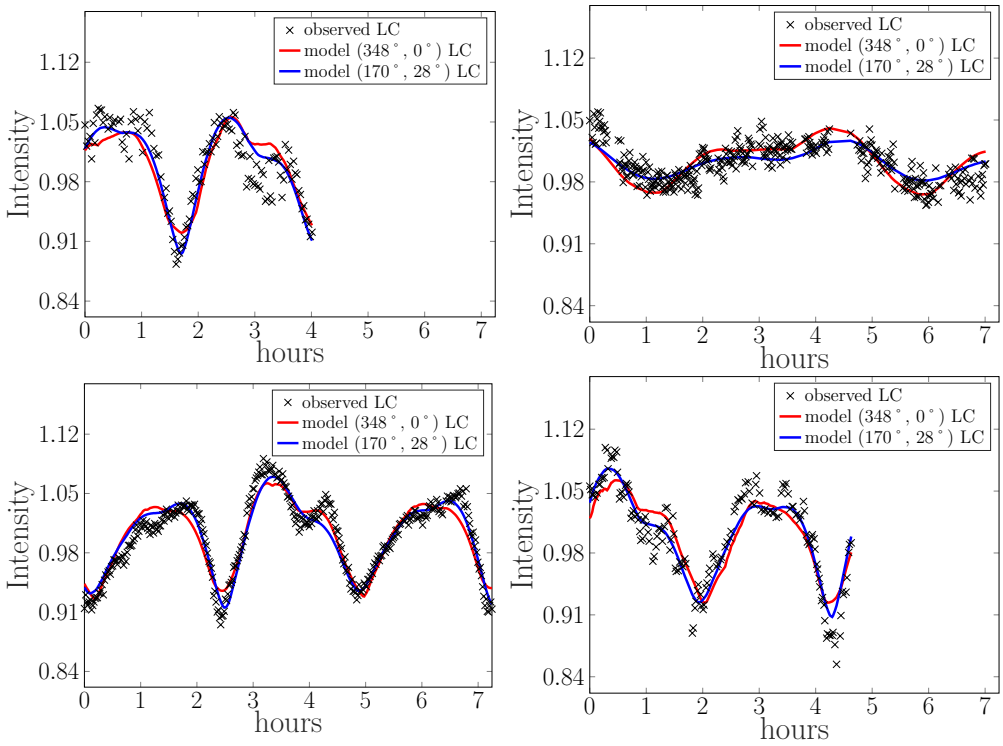

Figure 4.45: Four exemplar light curves of asteroid (423) Diotima with two models' fit. The model $(348°, 1°)$ fits the data better.

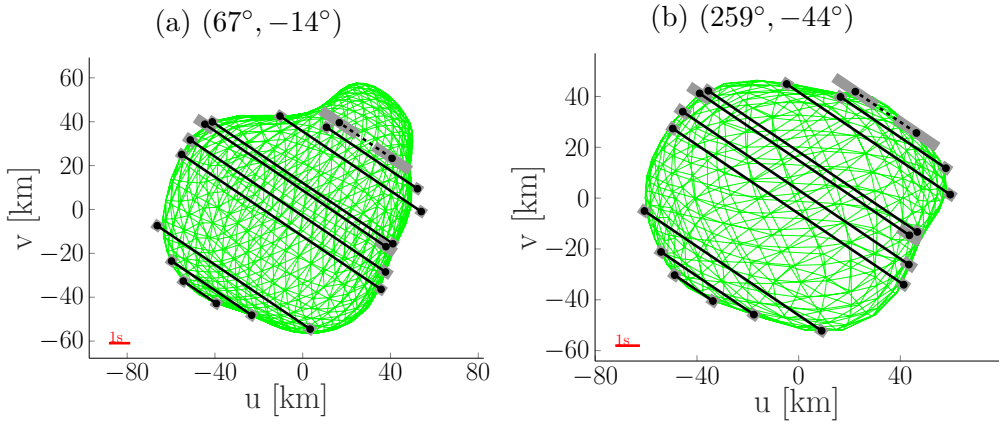

Figure 4.46: Two models of asteroid (506) Marion from ADAM with projections to occultation. Neither of the model fits the data sufficiently enough.

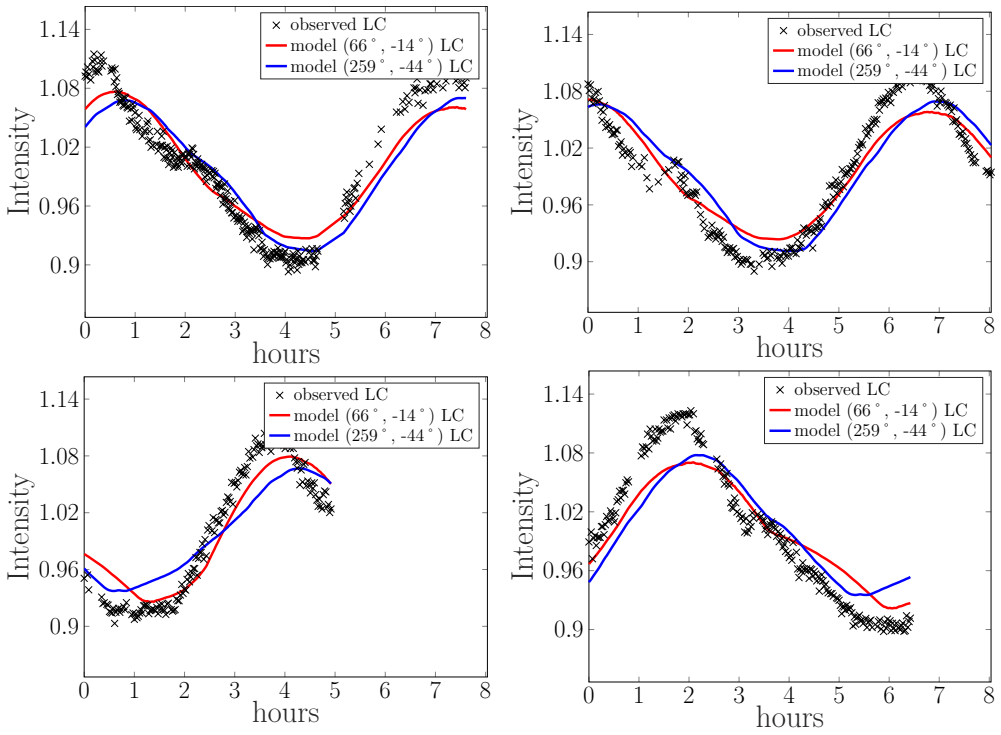

Figure 4.47: Four exemplar light curves of asteroid (506) Marion with two models' fit. Neither of the model fits the data sufficiently enough.

fit to one data worsen the fit on the other. The fit to light curves is better for convex model, which on the other does not fit the occultations. And if we want to fit also the occultations, fit to light curves is worse. Finding period and poles also suggest the insufficiency of the data. We get a global minimum of period of 37.19 h and another local 37.18 h with only slightly bigger value and for each of these periods I found 5 pole positions. Surprisingly, I have come to conclusion, that the period 37.18 is the correct one. Because after creating several models almost all of them corresponded to the occultations, but the ones with smaller period have much better fit of light curves. From these models I have finally chose one with pole position $(259°, 26°)$. There is another model that fits the data only slightly worst and that is with pole position $(173°, -12°)$. Fit of these two models to light curves is shown in Fig. 4.49 and to occultations in Fig. 4.48.

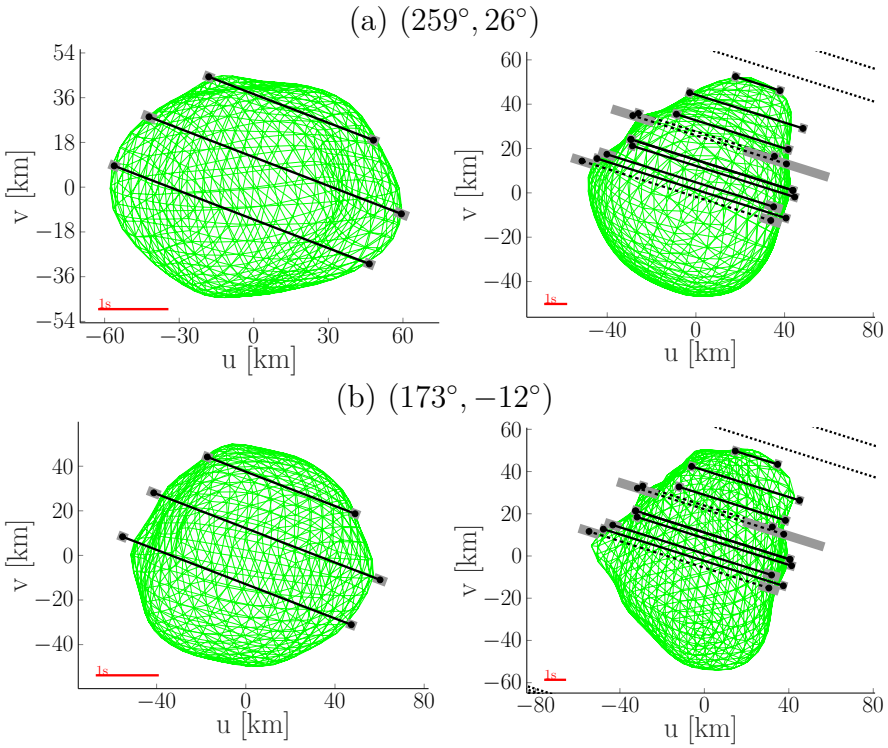

Figure 4.48: Two models of asteroid (788) Hohensteina from ADAM with projections to two occultations. Neither of the model fits the data sufficiently enough.

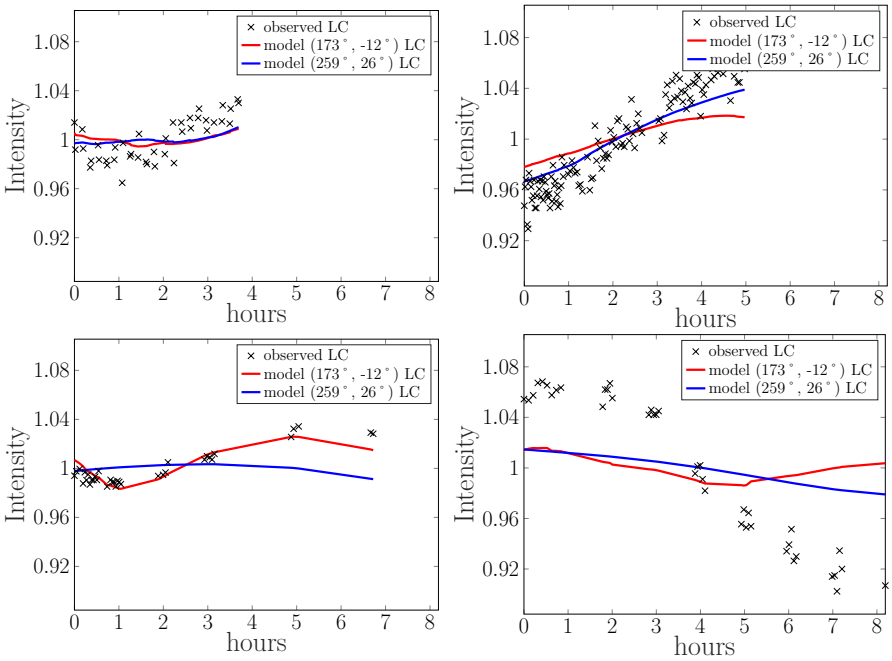

Figure 4.49: Four exemplar light curves of asteroid (788) Hohensteina with two models' fit. Neither of the model fits the data sufficiently enough.

Conclusion

Most asteroid models have been derived from light curves alone. These models are convex and not scaled. Only some of these asteroids have other observations available, like observations with adaptive optics or direct observations from spacecraft, which are disc-resolved. For the rest of the asteroids, we do not have a way of identifying non-convex asteroids and determining their precise dimension, apart from observations in IR, which depend on thermal models. This leaves us with occultations as a direct method for size determination.

Occultations are a useful tool for asteroid observations because we can determine precise dimensions and non-convexity of even kilometer–sized asteroids. But to get this information we need enough and well-distributed observers. Only in recent years has the number of occultation observations with lots of observers increased to cover enough asteroids for more common usage. Therefore most occultation observations are unused in modelling and asteroid models are still done without them. In this thesis, I change this.

In my bachelor thesis, I processed all available data from occultations and chose asteroids with an occultation containing at least three chords. For all of those asteroids, I have compared these occultations with their models from DAMIT (if there are any). This gave me 274 asteroids whose model I scaled to occultation. This way I was able to determine asteroids' precise dimensions, solve the pole ambiguity and find non-corresponding shape solutions.

In this work, I created a new model for those asteroids that have no previous model or non-fitting one. This gave me 34 asteroids for which I have created a new model using both light curves and occultations. Almost all of these asteroids had more possible pole positions derived from light curves alone. However, with the usage of occultations in shape modelling, I was able to determine which of those positions was correct for almost all of these asteroids. This was done based on the models' fit to observed light curves and occultations. This gave me 33 asteroids, which now have improved models than before or new models if they had none. These models will be published in a paper and added to DAMIT along with their dimensions and data set.

I have also created a way to process all occultation observations that will become available in the future. This rate is currently at over a thousand events per year and is expected to increase. Even if most of these occultations have too few observers to be used in Shape determination, there are still lots of events that can be useful. Therefore, occultation will be able to play a bigger role in our study of asteroids. Not only because their observations are easier than most others, like adaptive optics, but they have higher spatial precision. Observations of the occultation can give spatial resolution in the order of kilometres for every asteroid. Therefore, they surpass any other available observations except for direct spacecraft observations.

Thanks to occultations, we will be able to determine more details in shape and determine their dimensions more precisely. All of this is important to understand processes which shaped our Solar System and have an impact on the movement of celestial bodies and planetary system formation. Especially non-convex models that can show post–impact features like craters and matter accretion. From

these features, it is possible to determine the collision history of asteroids and their initial population. Even tracing the creation of asteroid families is based on identifying the parent body that underwent a collision. All of this can help us to understand the collision processes of celestial bodies.

Bibliography

Arimatsu, K., Tsumura, K., Usui, F., et al. A kilometre-sized Kuiper belt object discovered by stellar occultation using amateur telescopes. *Nature Astronomy*, 3:301–306, January 2019. doi: 10.1038/s41550-018-0685-8.

Bottke, William F., J., Vokrouhlický, D., Rubincam, D. P., Nesvorný, D. The Yarkovsky and Yorp Effects: Implications for Asteroid Dynamics. *Annual Review of Earth and Planetary Sciences*, 34:157–191, May 2006. doi: 10.1146/annurev.earth.34.031405.125154.

Camargo, J. I. B., Banda-Huarca, M. V., Ogando, R. L., et al. Solar system astrometry, Gaia, and the large surveys - a huge step ahead to stellar occultations by distant small solar system bodies. In Recio-Blanco, A., de Laverny, P., Brown, A. G. A., Prusti, T., editors, *Astrometry and Astrophysics in the Gaia Sky*, volume 330, pages 397–398, April 2018. doi: 10.1017/S1743921317005488.

Černý, D. Zákryty hvězd planetkami, 2022. Bachelor thesis, Charles University, Faculty of mathematics and physics, Astronomical institute. Superviser Ďurech, Josef.

Delbo, M., Mueller, M., Emery, J. P., Rozitis, B., Capria, M. T. Asteroid Thermophysical Modeling. In *Asteroids IV*, pages 107–128. 2015. doi: 10.2458/azu_uapress_9780816532131-ch006.

Dong, S., Shappee, B. J., Prieto, J. L., et al. ASASSN-15lh: A highly superluminous supernova. *Science*, 351(6270):257–260, January 2016. doi: 10.1126/science.aac9613.

Elliot, J. L., Dunham, E., Wasserman, L. H., Millis, R. L., Churms, J. The radii of Uranian rings alpha , beta , gamma , delta , epsilon , eta , 4, 5, and 6 from their occultations of SAO 158687. AJ, 83:980–992, August 1978. doi: 10.1086/112280.

Ferreira, J. F., Tanga, P., Spoto, F., Machado, P., Herald, D. Asteroid astrometry by stellar occultations: Accuracy of the existing sample from orbital fitting. A&A, 658:A73, February 2022. doi: 10.1051/0004-6361/202141753.

Gaia Collaboration, Prusti, T., de Bruijne, J. H. J., et al. The Gaia mission. A&A, 595:A1, November 2016. doi: 10.1051/0004-6361/201629272.

Gaia Collaboration, Brown, A. G. A., Vallenari, A., et al. Gaia Early Data Release 3. Summary of the contents and survey properties. A&A, 649:A1, May 2021. doi: 10.1051/0004-6361/202039657.

Gault, D., Nosworthy, P., Nolthenius, R., Bender, K., Herald, D. A New Satellite of 4337 Arecibo Detected and Confirmed by stellar Occultation. *Minor Planet Bulletin*, 49(1):3–5, January 2022.

Harris, A. W. A Thermal Model for Near-Earth Asteroids. Icarus, 131(2):291–301, February 1998. doi: 10.1006/icar.1997.5865.

Herald, D., Gault, D., Anderson, R., et al. Precise astrometry and diameters of asteroids from occultations - a data set of observations and their interpretation. MNRAS, 499(3):4570–4590, December 2020. doi: 10.1093/mnras/staa3077.

Holsapple, K. A. Main belt asteroid collision histories: Cratering, ejecta, erosion, catastrophic dispersions, spins, binaries, tops, and wobblers. Planet. Space Sci., 219:105529, September 2022. doi: 10.1016/j.pss.2022.105529.

Ivezić, Ž., Kahn, S. M., Tyson, J. A., et al. LSST: From Science Drivers to Reference Design and Anticipated Data Products. ApJ, 873(2):111, March 2019. doi: 10.3847/1538-4357/ab042c.

Kaasalainen, M. Torppa, J. Optimization Methods for Asteroid Lightcurve Inversion. I. Shape Determination. Icarus, 153(1):24–36, September 2001. doi: 10.1006/icar.2001.6673.

Kaasalainen, M., Torppa, J., Muinonen, K. Optimization Methods for Asteroid Lightcurve Inversion. II. The Complete Inverse Problem. Icarus, 153(1):37–51, September 2001. doi: 10.1006/icar.2001.6674.

Kaasalainen, M. Lamberg, L. Inverse problems of generalized projection operators. *Inverse Problems*, 22(3):749–769, June 2006. doi: 10.1088/0266-5611/22/3/002.

Lebofsky, L. A., Sykes, M. V., Tedesco, E. F., et al. A refined "standard" thermal model for asteroids based on observations of 1 Ceres and 2 Pallas. Icarus, 68 (2):239–251, November 1986. doi: 10.1016/0019-1035(86)90021-7.

Lin, C.-L., Zhang, Z.-W., Chen, W. P., et al. A Close Binary Star Resolved from Occultation by 87 Sylvia. PASP, 121(878):359, April 2009. doi: 10.1086/598968.

Magri, C., Nolan, M. C., Ostro, S. J., Giorgini, J. D. A radar survey of main-belt asteroids: Arecibo observations of 55 objects during 1999 2003. Icarus, 186(1): 126–151, January 2007. doi: 10.1016/j.icarus.2006.08.018.

Mainzer, A. K., Bauer, J. M., Cutri, R. M., et al. NEOWISE Diameters and Albedos V2.0. NASA Planetary Data System, urn:nasa:pds:neowise_diameters_albedos::2.0, January 2019.

Marciniak, A., Ďurech, J., Choukroun, A., et al. Scaling slowly rotating asteroids with stellar occultations. A&A, 679:A60, November 2023. doi: 10.1051/0004-6361/202346191.

Mignard, F., Bailer-Jones, C., Bastian, U., et al. Gaia: organisation and challenges for the data processing. In Jin, W. J., Platais, I., Perryman, M. A. C., editors, *A Giant Step: from Milli- to Micro-arcsecond Astrometry*, volume 248, pages 224–230, July 2008. doi: 10.1017/S1743921308019145.

Millis, R. L., Wasserman, L. H., Franz, O. G., et al. Pluto's Radius and Atmosphere: Results from the Entire 9 June 1988 Occultation Data Set. Icarus, 105 (2):282–297, October 1993. doi: 10.1006/icar.1993.1126.

Morbidelli, A. Vokrouhlický, D. The Yarkovsky-driven origin of near-Earth asteroids. Icarus, 163(1):120–134, May 2003. doi: 10.1016/S0019-1035(03)00047-2.

Novaković, B., Vokrouhlický, D., Spoto, F., Nesvorný, D. Asteroid families: properties, recent advances, and future opportunities. *Celestial Mechanics and Dynamical Astronomy*, 134(4):34, August 2022. doi: 10.1007/s10569-022-10091-7.

Roques, F. Moncuquet, M. A Detection Method for Small Kuiper Belt Objects: The Search for Stellar Occultations. Icarus, 147(2):530–544, October 2000. doi: 10.1006/icar.2000.6452.

Saint-Pe, O., Combes, M., Rigaut, F., Tomasko, M., Fulchignoni, M. Demonstration of Adaptive Optics for Resolved Imagery of Solar System Objects: Preliminary Results on Pallas and Titan. Icarus, 105(2):263–270, October 1993. doi: 10.1006/icar.1993.1124.

Tanga, P., Pauwels, T., Mignard, F., et al. Gaia Data Release 3. The Solar System survey. A&A, 674:A12, June 2023. doi: 10.1051/0004-6361/202243796.

Tonry, J. L. An Early Warning System for Asteroid Impact. PASP, 123(899):58, January 2011. doi: 10.1086/657997.

Viikinkoski, M., Kaasalainen, M., Durech, J. ADAM: a general method for using various data types in asteroid reconstruction. A&A, 576:A8, April 2015. doi: 10.1051/0004-6361/201425259.

Warner, B. D., Stephens, R. D., Harris, A. W. Save the Lightcurves. *Minor Planet Bulletin*, 38(3):172–174, July 2011.

Ďurech, J., Kaasalainen, M., Herald, D., et al. Combining asteroid models derived by lightcurve inversion with asteroidal occultation silhouettes. Icarus, 214(2):652–670, August 2011. doi: 10.1016/j.icarus.2011.03.016.